BS EN IEC/IEEE 63184:2025

BSI Standards Publication

Assessment methods of the human exposure to electric and magnetic fields from wireless power transfer systems — Models, instrumentation, measurement and computational methods and procedures (frequency range of 3 kHz to 30 MHz)

Documents
Document Sharing Hub

Full document details: BS EN IEC/IEEE 63184:2025

National foreword

This British Standard is the UK implementation of EN IEC/IEEE 63184:2025. It is identical to IEC/IEEE 63184:2025.

The UK participation in its preparation was entrusted to Technical Committee GEL/106, Human exposure to low frequency and high frequency electromagnetic radiation.

A list of organizations represented on this committee can be obtained on request to its committee manager.

Contractual and legal considerations

This publication has been prepared in good faith, however no representation, warranty, assurance or undertaking (express or implied) is or will be made, and no responsibility or liability is or will be accepted by BSI in relation to the adequacy, accuracy, completeness or reasonableness of this publication. All and any such responsibility and liability is expressly disclaimed to the full extent permitted by the law.

This publication is provided as is, and is to be used at the recipient's own risk.

The recipient is advised to consider seeking professional guidance with respect to its use of this publication.

This publication is not intended to constitute a contract. Users are responsible for its correct application.

© The British Standards Institution 2025
Published by BSI Standards Limited 2025

ISBN 978 0 580 99999 4

ICS 17.220.20; 17.240

Compliance with a British Standard cannot confer immunity from legal obligations.

This British Standard was published under the authority of the Standards Policy and Strategy Committee on 30 April 2025.

Amendments/corrigenda issued since publication

Date	Text affected

Documents
Document Sharing Hub

Full document details: BS EN IEC/IEEE 63184:2025

EUROPEAN STANDARD

NORME EUROPÉENNE

EUROPÄISCHE NORM

EN IEC/IEEE 63184

April 2025

ICS 17.220.20; 17.240

English Version

Assessment methods of the human exposure to electric and magnetic fields from wireless power transfer systems - Models, instrumentation, measurement and computational methods and procedures (frequency range of 3 kHz to 30 MHz) (IEC/IEEE 63184:2025)

Méthodes d'évaluation de l'exposition humaine aux champs électriques et magnétiques produits par les systèmes de transfert de puissance sans fil - Modèles, instrumentation, méthodes et procédures de mesure et de calcul (Plage de fréquences comprise entre 3 kHz et 30 MHz) (IEC/IEEE 63184:2025)

Bewertungsmethoden für die Exposition des Menschen gegenüber elektrischen und magnetischen Feldern von drahtlosen Energieübertragungssystemen - Modelle, Instrumente, Mess- und Berechnungsmethoden und -verfahren (Frequenzbereich von 3 kHz bis 30 MHz) (IEC/IEEE 63184:2025)

This European Standard was approved by CENELEC on 2025-04-01. CENELEC members are bound to comply with the CEN/CENELEC Internal Regulations which stipulate the conditions for giving this European Standard the status of a national standard without any alteration.

Up-to-date lists and bibliographical references concerning such national standards may be obtained on application to the CEN-CENELEC Management Centre or to any CENELEC member.

This European Standard exists in three official versions (English, French, German). A version in any other language made by translation under the responsibility of a CENELEC member into its own language and notified to the CEN-CENELEC Management Centre has the same status as the official versions.

CENELEC members are the national electrotechnical committees of Austria, Belgium, Bulgaria, Croatia, Cyprus, the Czech Republic, Denmark, Estonia, Finland, France, Germany, Greece, Hungary, Iceland, Ireland, Italy, Latvia, Lithuania, Luxembourg, Malta, the Netherlands, Norway, Poland, Portugal, Republic of North Macedonia, Romania, Serbia, Slovakia, Slovenia, Spain, Sweden, Switzerland, Türkiye and the United Kingdom.

European Committee for Electrotechnical Standardization
Comité Européen de Normalisation Electrotechnique
Europäisches Komitee für Elektrotechnische Normung

CEN-CENELEC Management Centre: Rue de la Science 23, B-1040 Brussels

© 2025 CENELEC All rights of exploitation in any form and by any means reserved worldwide for CENELEC Members.

Ref. No. EN IEC/IEEE 63184:2025 E

Documents
Document Sharing Hub

Full document details: BS EN IEC/IEEE 63184:2025

European foreword

The text of document 106/669/FDIS, future edition 1 of IEC/IEEE 63184, prepared by TC 106 "Methods for the assessment of electric, magnetic and electromagnetic fields associated with human exposure" was submitted to the IEC-CENELEC parallel vote and approved by CENELEC as EN IEC/IEEE 63184:2025.

The following dates are fixed:

- latest date by which the document has to be implemented at national level by publication of an identical national standard or by endorsement (dop) 2026-04-30
- latest date by which the national standards conflicting with the document have to be withdrawn (dow) 2028-04-30

Attention is drawn to the possibility that some of the elements of this document may be the subject of patent rights. CENELEC shall not be held responsible for identifying any or all such patent rights.

Any feedback and questions on this document should be directed to the users' national committee. A complete listing of these bodies can be found on the CENELEC website.

Endorsement notice

The text of the International Standard IEC/IEEE 63184:2025 was approved by CENELEC as a European Standard without any modification.

In the official version, for Bibliography, the following notes have to be added for the standard indicated:

IEC 61980-3:2022	NOTE	Approved as EN IEC 61980-3:2022 (not modified)
IEC 62226-2-1:2004	NOTE	Approved as EN 62226-2-1:2005 (not modified)
IEC 62233:2005	NOTE	Approved as EN 62233:2008
IEC 62311:2019	NOTE	Approved as EN IEC 62311:2020 (not modified)
IEC 60990:2016	NOTE	Approved as EN 60990:2016 (not modified)
IEC/IEEE 63195-2:2022	NOTE	Approved as EN IEC/IEEE 63195-2:2023 (not modified)
ISO/IEC 17025:2017	NOTE	Approved as EN ISO/IEC 17025:2017 (not modified)
ISO 19363:2020	NOTE	Approved as EN ISO 19363:2021 (not modified)

Documents
Document Sharing Hub

Full document details: BS EN IEC/IEEE 63184:2025

Annex ZA
(normative)

Normative references to international publications with their corresponding European publications

The following documents are referred to in the text in such a way that some or all of their content constitutes requirements of this document. For dated references, only the edition cited applies. For undated references, the latest edition of the referenced document (including any amendments) applies.

NOTE 1 Where an International Publication has been modified by common modifications, indicated by (mod), the relevant EN/HD applies.

NOTE 2 Up-to-date information on the latest versions of the European Standards listed in this annex is available here: www.cencenelec.eu.

Publication	Year	Title	EN/HD	Year
IEC 61786-1	2013	Measurement of DC magnetic, AC magnetic and AC electric fields from 1 Hz to 100 kHz with regard to exposure of human beings - Part 1: Requirements for measuring instruments	EN 61786-1	2014
+ AMD1	2024		+ A1	2024
IEC 61786-2	2014	Measurement of DC magnetic, AC magnetic and AC electric fields from 1 Hz to 100 kHz with regard to exposure of human beings - Part 2: Basic standard for measurements	-	-
IEC/IEEE 62209-1528	2020	Measurement procedure for the assessment of specific absorption rate of human exposure to radio frequency fields from hand-held and body-worn wireless communication devices - Part 1528: Human models, instrumentation and procedures (Frequency range of 4 MHz to 10 GHz)	EN IEC/IEEE 62209-1528	2021
IEC/IEEE 62704-1	2017	Determining the peak spatial-average specific absorption rate (SAR) in the human body from wireless communications devices, 30 MHz to 6 GHz - Part 1: General requirements for using the finite difference time-domain (FDTD) method for SAR calculations 	-	-
IEC/IEEE 62704-4	2020	Determining the peak spatial-average specific absorption rate (SAR) in the human body from wireless communication devices, 30 MHz to 6 GHz - Part 4: General requirements for using the finite element method for SAR calculations	-	-

Documents
Document Sharing Hub

Full document details: BS EN IEC/IEEE 63184:2025

CONTENTS

FOREWORD 10
INTRODUCTION 12
1 Scope 13
2 Normative references 13
3 Terms and definitions 14
4 Symbols and abbreviated terms 19
4.1 Physical quantities 19
4.2 Constants 19
4.3 Abbreviated terms 19
5 Assessment procedures 20
5.1 General 20
5.2 Compliance assessment considering direct effects 21
5.2.1 General 21
5.2.2 Tier 1: Evaluation based on coil current 22
5.2.3 Tier 2: Evaluation of incident fields against reference levels 23
5.2.4 Tier 3: Evaluation of incident magnetic fields using coupling factor 23
5.2.5 Tier 4: Evaluation of internal E-field, current density, or SAR against basic restrictions 29
5.3 Exposure assessment of contact currents 29
6 Measurement methods 31
6.1 Incident fields 31
6.1.1 General 31
6.1.2 Equipment 32
6.2 SAR and pE_{ind} 34
6.3 Contact currents 36
6.3.1 General 36
6.3.2 Equipment 36
6.3.3 Measurements 37
7 Computational assessment methods 38
7.1 General 38
7.2 Quasi-static approximation 39
7.3 Computational assessment against the basic restrictions 40
7.3.1 General 40
7.3.2 Peak spatial-average SAR 41
7.3.3 Whole-body average SAR 41
7.3.4 Averaged current density on a surface 41
7.3.5 Peak spatial average internal E-field in a cubical volume 41
7.3.6 Peak spatial average internal E-field along a line 41
7.3.7 Maximum local internal E-field 41
8 Combination of measurement and computational methods for inductive WPT systems 42
8.1 General 42
8.2 Measurement of magnetic field 42
8.3 Computational analyses of induced quantities 42
8.4 Computational assessment against the basic restrictions 43
9 Uncertainty assessments 43

AVA Documents
Document Sharing Hub
Full document details: BS EN IEC/IEEE 63184:2025

9.1 General ... 43
9.2 Measurement methods ... 43
9.2.1 Measurement uncertainty budget ... 43
9.2.2 Amplitude calibration uncertainty ... 44
9.2.3 Probe anisotropy ... 45
9.2.4 Probe dynamic range linearity ... 45
9.2.5 Probe frequency domain response ... 45
9.2.6 Modulation response ... 45
9.2.7 Spatial averaging (maximum gradient) ... 45
9.2.8 Gradient assessment uncertainty ... 45
9.2.9 Parasitic E-field and H-field sensitivity ... 45
9.2.10 Detection limit ... 45
9.2.11 Readout electronics ... 46
9.2.12 Response time ... 46
9.2.13 Probe positioning ... 46
9.2.14 Signal postprocessing ... 46
9.2.15 Nominal position ... 46
9.2.16 Repeatability ... 46
9.2.17 DUT ... 46
9.3 Computational methods ... 46
9.3.1 Computational uncertainty budget ... 46
9.3.2 Grid resolution ... 48
9.3.3 Tissue parameters ... 48
9.3.4 Exposure position ... 48
9.3.5 Convergence ... 48
9.3.6 Power budget ... 49
9.3.7 Boundary conditions ... 49
9.3.8 Quasi-static approximation ... 49
9.3.9 Model parts and geometry ... 49
9.3.10 Dielectric parameters ... 49
9.3.11 Ferrite parameters ... 50
9.3.12 Positioning of transmit and receive coils ... 50
9.3.13 Coupling of transmit and receive coils ... 50
9.3.14 Exposure sources other than the coils ... 50
9.3.15 Loading of the coil ... 50
9.4 Assessment of combining measurement and computational methods ... 50
10 Reporting ... 51
10.1 General ... 51
10.2 Items to be recorded in exposure compliance assessment reports ... 51
10.3 Additional items to be included for evaluation measurements ... 52
10.4 Additional items to be included for numerical and combined numerical and measurement evaluations ... 53
Annex A (normative) Exposure evaluations using approximations ... 54
A.1 Limit on current for a WPT coil ... 54
A.2 Induced field quantities for comparison with basic restrictions ... 55
A.3 Enhancement or coverage factor ... 57
Annex B (normative) Calibration methods ... 58
B.1 General ... 58
B.2 E-field and H-field calibration ... 58

AVA Documents
Document Sharing Hub
Full document details: BS EN IEC/IEEE 63184:2025

B.2.1 Standard field generation methods 58
B.2.2 Characteristics to be measured 58
B.2.3 Frequency domain calibration 60
B.2.4 E-field calibration 63
B.3 Gradient response verification 67
B.3.1 General 67
B.3.2 H-field gradient verification: Main steps 67
B.3.3 Uncertainty for H-field gradient verification 67
B.4 Dosimetric probe calibration 68
B.4.1 General 68
B.4.2 Calibration with short dipole antennas via transmit antenna factor 69
B.4.3 Uncertainty 72
Annex C (normative) Verification and validation methods for measurements 73
C.1 General 73
C.2 Objective 73
C.3 Measurement setup and procedure for system verification and system validation 73
C.3.1 General 73
C.3.2 Measurement system verification: test procedure 74
C.3.3 Measurement system validation: test procedure 75
Annex D (informative) Case study on the dependency of SAR on phantom properties and size 76
D.1 Phantom properties 76
D.2 Phantom size 79
Annex E (informative) Extrapolation methods of SAR measurement 82
E.1 General 82
E.2 Measurement and interpolation of electric field inside a phantom 82
E.2.1 General 82
E.2.2 Extrapolation functions 82
E.2.3 Three steps for determination of spatial-peak SAR 83
E.2.4 Validation of measurement methods using extrapolation 83
E.2.5 Uncertainty 86
Annex F (informative) Computational methods 88
F.1 General 88
F.2 Quasi-static finite element method 88
F.3 Scalar potential finite difference method 89
F.4 Impedance method 90
F.5 Finite-difference time-domain method 91
F.6 Hybrid technique of MoM and FDTD method 91
F.7 Hybrid technique of FEM and SPFD method 93
Annex G (informative) Averaging algorithms 94
G.1 Current density averaging over an area 94
G.1.1 General 94
G.1.2 Calculation of the current density in a Cartesian voxel 94
G.1.3 Calculation of the current density in a tetrahedron 95
G.1.4 Calculation of J_{av} 95
G.2 Internal E-field 96
G.2.1 General 96

AVA Documents
Document Sharing Hub
Full document details: BS EN IEC/IEEE 63184:2025

G.2.2 E-field averaging in a cubical volume 96
G.2.3 E-field averaging along an averaging distance 97
G.2.4 Maximum local E-field 99
Annex H (normative) Code verification and model validations 100
H.1 Code verification 100
H.1.1 General 100
H.1.2 Quasi-static codes 100
H.1.3 Quasi-static codes for the calculation of the incident magnetic field 101
H.1.4 Averaging algorithms 103
H.2 Model validation 104
H.2.1 General 104
H.2.2 Recommendations for the development of the computational model 105
H.2.3 Determining the validity of the field source 105
Annex I (informative) Use cases of magnetic field exposure assessment 107
I.1 EV WPT – electric passenger car 107
I.1.1 General 107
I.1.2 Determination of user position 107
I.1.3 Assessment procedures considering direct effects for WPT system for EV 108
I.1.4 Assessment procedures for contact currents of WPT systems for EV 114
I.2 Heavy duty vehicle EMF measurement procedure 119
I.2.1 General 119
I.2.2 Step 1 119
I.2.3 Step 2 121
I.2.4 Step 3 121
I.3 Remotely piloted aircraft 122
I.3.1 General 122
I.3.2 Assessment procedures of WPT system for RPA 122
Annex J (informative) Examples of magnetic field exposure assessment 126
J.1 General 126
J.2 Assessment procedure of heavy-duty WPT EV system 126
J.2.1 Outline of assessment procedure 126
J.2.2 Test condition 126
J.2.3 Test result 1 127
J.2.4 Test result 2 127
J.2.5 Test result 3 127
J.3 Remotely piloted aircraft 127
J.3.1 General 127
J.3.2 Description of WPT system for RPA 128
J.3.3 Measurement of magnetic field around the WPT system for RPA 128
J.3.4 Modelling for the WPT system for RPA 129
J.3.5 Evaluation of incident field against basic restrictions 129
J.3.6 Evaluation of current density, internal electric field, and SAR against basic restrictions 132
J.4 Combined method of measurement and computational analysis 132
J.4.1 General 132
J.4.2 Measurement of magnetic field 132
J.4.3 Computational analyses of induced quantities 133
J.4.4 Example of exposure assessment for WPT systems using combined method 133

AVA Documents
Document Sharing Hub

J.5 SAR measurement for WPT system 137
Annex K (informative) Proximity detection sensor considerations for exposure assessment 139
K.1 General 139
K.2 Phantom specification 139
K.2.1 Phantom for the stationary living object detection 139
K.2.2 Phantom for the proximity living object detection 139
K.3 Procedures for determining proximity detection sensor triggering distance 140
K.4 Testing areas 140
K.5 Procedures for determining stationary living objects 141
Bibliography 143

Figure 1 – Flowchart for the assessment procedure 20
Figure 2 – Flowchart for the assessment procedure considering direct effects 21
Figure 3 – The gradient G_n is determined at the surface and normal to the surface, i.e. in the direction of the axis shown 26
Figure 4 – Coupling factors k of Formula (7) through Formula (11) as a function of the normalized magnetic field gradient [13] 29
Figure 5 – Two exposure situations for ungrounded and grounded metal objects 30
Figure 6 – Flowchart for assessment procedures for contact currents 31
Figure 7 – Human body equivalent circuit proposed in IEC 60990 [30] 37
Figure 8 – Impedance frequency characteristics of adult male and equivalent circuits proposed in IEC 60990 [30] and evaluated values [31], [32], [33], [34] 37
Figure 9 – Example of contact current measurement equipment 37
Figure A.1 – Comparison of the H-field with number of turns n at 1 cm from a circular coil calculated with Biot-Savart and with the approximation of Formula (A.1) 55
Figure B.1 – H-field and E-field generation setup for probe calibration 60
Figure B.2 – H-field generation setup for dynamic range calibration 62
Figure B.3 – E-field generation setup for frequency response calibration 64
Figure B.4 – E-field generation setup for dynamic range calibration 65
Figure B.5 – Illustration of the transmit antenna factor evaluation setup [51] 71
Figure B.6 – Illustration of the sensitivity coefficients evaluation setup [51] 71
Figure C.1 – Recommended test setups for measurement system verification and validation 74
Figure D.1 – Simulation model of large WPT system operating close to a) elliptical phantom and b) human body model 77
Figure D.2 – Different exposure conditions for human body model 77
Figure D.3 – Calculated SAR for circular coils with a 50 cm diameter operating at 6 cm from the elliptical phantom and heterogeneous human model 78
Figure D.4 – Simulation model of small WPT system operating close to a) elliptical phantom and b) human body model 78
Figure D.5 – Calculated SAR for the small square coils with dimensions 10 cm × 10 cm operating at 2 cm from the elliptical phantom and heterogeneous human model 79
Figure D.6 – Layout of large WPT system for exposure condition of a) case A and b) case C with respect to the elliptical phantom surface 80

Documents
Document Sharing Hub
Full document details: BS EN IEC/IEEE 63184:2025

Figure D.7 – Calculated 10 g-averaged SAR versus the smaller axis of elliptical phantom v normalized by coil outer diameter D for a) case A (f_{high} = 7,54 MHz) and b) case C (f_{low} = 6,14 MHz, f_{high} = 7,18 MHz) 80

Figure D.8 – Layout of small WPT system for exposure conditions of case C with respect to a) elliptical phantom and b) rectangular phantom 81

Figure D.9 – Calculated 10 g-averaged SAR versus the smaller axis v or width W normalized by square coil diagonal K for a) elliptical phantom (f_{low} = 6,6 MHz, f_{high} = 7,64 MHz) and b) rectangular phantom (f_{low} = 6,59 MHz) 81

Figure E.1 – Schematic diagram of measurement system 84

Figure E.2 – Measurement system 85

Figure E.3 – Measured and simulated electric field distributions in the measurement plane 25 mm away from the phantom boundary with solenoid-type WPT system positioned parallel to the phantom wall 85

Figure E.4 – Measured and simulated electric field distributions in the measurement plane 25 mm away from the phantom boundary with flat-spiral-type WPT system positioned parallel to the phantom wall 86

Figure E.5 – 10 g averaged SAR obtained by measurement, and extrapolation and MoM-derived 10 g averaged SAR 86

Figure G.1 – Field components on voxel edges 95

Figure H.1 – Coordinate system and angles 102

Figure I.1 – Example for regions of protection, for ground mounted systems (vehicle) [78] 107

Figure I.2 – Example for regions of protection, for ground mounted systems (using vehicle mimic plate) 108

Figure I.3 – Flowchart for EV and vehicle mimic plate assessment (direct effect) 109

Figure I.4 – Region 2 measurement positions (WPT) 110

Figure I.5 – Region 3 measurement positions 111

Figure I.6 – Region 2 measurement positions of vehicle mimic plate (WPT) 112

Figure I.7 – Region 3 measurement positions of vehicle mimic plate (WPT) 113

Figure I.8 – Flowchart for EV use and vehicle mimic plate assessment (contact currents) 114

Figure I.9 – Configuration example of contact current with grounded condition: (1) with vehicle 116

Figure I.10 – Configuration example of contact current with grounded condition: (2) with vehicle mimic plate 116

Figure I.11 – Configuration example of contact current with ungrounded condition: (1) with vehicle 118

Figure I.12 – Configuration example of contact current with ungrounded condition: (2) with vehicle mimic plate 119

Figure I.13 – EMF measurement for heavy duty vehicle: top view 120

Figure I.14 – EMF measurement for heavy duty vehicle: side view 120

Figure I.15 – Measurement points on the inside floor of WPT bus 121

Figure I.16 – Measurement position 123

Figure J.1 – EMF test of an electric bus (2015 August 7, Sejong City) 126

Figure J.2 – Test result 1 from side-view 127

Figure J.3 – Geometry and measurement position of WPT system for RPA 128

Documents
Document Sharing Hub

Full document details: BS EN IEC/IEEE 63184:2025

Figure J.4 – Measured magnetic field strength 129
Figure J.5 – Measured and computed magnetic field strength 129
Figure J.6 – Measurement system for the magnetic near-field of WPT systems [83] 133
Figure J.7 – Schematic view and picture of the fabricated magnetic-field probes [83] 133
Figure J.8 – Schematic view (left) and picture (right) of WPT systems [83] 135
Figure J.9 – Exposure conditions for WPT coils [83] 135
Figure J.10 – Amplitude and phase distributions of magnetic fields measured near WPT systems without (w/o) and with (w/) ferrite tiles [83] 136
Figure J.11 – Distribution of the internal electric field strength with adult male model for an input power of 7,7 kW [83] 137
Figure J.12 – WPT system operating at 6,78 MHz 138
Figure J.13 – SAR distribution on a plane at 25 mm from the bottom of the phantom 138
Figure K.1 – Test side consideration drawing 141
Figure K.2 – Positioning of the phantom and the DUT WPT for determining the detection sensor triggering distance, an example of charging an electric vehicle with a WPT system 141

Table 1 – List of symbols used in the formulas of 5.2.4.2 and 5.2.4.3 24
Table 2 – Dielectric properties of the tissue-equivalent medium liquid 35
Table 3 – Dielectric properties of the tissue-equivalent medium NaCl solution of 0,074 mol/L 35
Table 4 – Computational methods 39
Table 5 – Example of uncertainty evaluation of the the E-field and H-field exposure assessment using measurement methods 43
Table 6 – Example of uncertainty evaluation of computational methods 47
Table 7 – Example of uncertainty evaluation of the exposure assessment combining measurements and computational methods 51
Table B.1 – EM field generation setups for probe and sensor calibrations 58
Table B.2 – Main components of H-field and E-field generation setups for frequency response calibration 60
Table B.3 – Template for uncertainty in frequency response calibration 61
Table B.4 – Main components of H-field generation setup for dynamic range calibration 62
Table B.5 – Template for uncertainty in H-field dynamic range calibration 62
Table B.6 – Main components of E-field generation setup for frequency response calibration 64
Table B.7 – Template for uncertainty in E-field frequency response calibration 64
Table B.8 – Main components of E-field generation setup for dynamic range calibration 65
Table B.9 – Template for the uncertainty of the E-field dynamic range 66
Table B.10 – Template for uncertainty of the H-field gradient verification 68
Table B.11 – Uncertainty template for evaluation of average internal electric field produced by short dipole antenna via transmit antenna factor 72
Table E.1 – Measurement uncertainty of 10 g averaged SAR 87
Table H.1 – Interpolation and superposition of vector field components for loop currents I and phase offsets ξ 103

Documents
Document Sharing Hub
Full document details: BS EN IEC/IEEE 63184:2025

Table J.1 – Computed coupling factor k_L 130

Table J.2 – Evaluation results using coupling factor k_L 130

Table J.3 – Evaluation results using coupling factor k_G 131

Table J.4 – Computational results of current density (J), internal electric field (E), and spatial peak 10 g average SAR ($SAR_{10\ g}$) 132

Documents
Document Sharing Hub

Full document details: BS EN IEC/IEEE 63184:2025

ASSESSMENT METHODS OF THE HUMAN EXPOSURE TO ELECTRIC AND MAGNETIC FIELDS FROM WIRELESS POWER TRANSFER SYSTEMS – MODELS, INSTRUMENTATION, MEASUREMENT AND COMPUTATIONAL METHODS AND PROCEDURES (FREQUENCY RANGE OF 3 kHz TO 30 MHz)

FOREWORD

1) The International Electrotechnical Commission (IEC) is a worldwide organization for standardization comprising all national electrotechnical committees (IEC National Committees). The object of IEC is to promote international co-operation on all questions concerning standardization in the electrical and electronic fields. To this end and in addition to other activities, IEC publishes International Standards, Technical Specifications, Technical Reports, Publicly Available Specifications (PAS) and Guides (hereafter referred to as "IEC document(s)"). Their preparation is entrusted to technical committees; any IEC National Committee interested in the subject dealt with may participate in this preparatory work. International, governmental and non-governmental organizations liaising with the IEC also participate in this preparation.

   IEEE Standards documents are developed within IEEE Societies and subcommittees of IEEE Standards Association (IEEE SA) Board of Governors. IEEE develops its standards through an accredited consensus development process, which brings together volunteers representing varied viewpoints and interests to achieve the final product. IEEE standards are documents developed by volunteers with scientific, academic, and industry-based expertise in technical working groups. Volunteers involved in technical working groups are not necessarily members of IEEE or IEEE SA and participate without compensation from IEEE. While IEEE administers the process and establishes rules to promote fairness in the consensus development process, IEEE does not independently evaluate, test, or verify the accuracy of any of the information or the soundness of any judgments contained in its standards.

   IEC collaborates closely with IEEE in accordance with conditions determined by agreement between the two organizations. This Dual Logo International Standard was jointly developed by the IEC and IEEE under the terms of that agreement.

2) The formal decisions of IEC on technical matters express, as nearly as possible, an international consensus of opinion on the relevant subjects since each technical committee has representation from all interested IEC National Committees. The formal decisions of IEEE on technical matters, once consensus within IEEE Societies and Standards Coordinating Committees has been reached, is determined by a balanced ballot of materially interested parties who indicate interest in reviewing the proposed standard. Final approval of the IEEE standards document is given by the IEEE Standards Association (IEEE SA) Standards Board.

3) IEC/IEEE Publications have the form of recommendations for international use and are accepted by IEC National Committees/IEEE Societies in that sense. While all reasonable efforts are made to ensure that the technical content of IEC/IEEE Publications is accurate, IEC or IEEE cannot be held responsible for the way in which they are used or for any misinterpretation by any end user.

4) In order to promote international uniformity, IEC National Committees undertake to apply IEC Publications (including IEC/IEEE Publications) transparently to the maximum extent possible in their national and regional publications. Any divergence between any IEC/IEEE Publication and the corresponding national or regional publication shall be clearly indicated in the latter.

5) IEC and IEEE do not provide any attestation of conformity. Independent certification bodies provide conformity assessment services and, in some areas, access to IEC marks of conformity. IEC and IEEE are not responsible for any services carried out by independent certification bodies.

6) All users should ensure that they have the latest edition of this publication.

7) No liability shall attach to IEC or IEEE or their directors, employees, servants or agents including individual experts and members of technical committees and IEC National Committees, or volunteers of IEEE Societies and the Standards Coordinating Committees of the IEEE Standards Association (IEEE SA) Standards Board, for any personal injury, property damage or other damage of any nature whatsoever, whether direct or indirect, or for costs (including legal fees) and expenses arising out of the publication, use of, or reliance upon, this IEC/IEEE Publication or any other IEC or IEEE Publications.

8) Attention is drawn to the normative references cited in this publication. Use of the referenced publications is indispensable for the correct application of this publication.

9) Attention is drawn to the possibility that implementation of this IEC/IEEE Publication may require use of material covered by patent rights. By publication of this standard, no position is taken with respect to the existence or validity of any patent rights in connection therewith. IEC or IEEE shall not be held responsible for identifying Essential Patent Claims for which a license may be required, for conducting inquiries into the legal validity or scope of Patent Claims or determining whether any licensing terms or conditions provided in connection with submission of a Letter of Assurance, if any, or in any licensing agreements are reasonable or non-discriminatory. Users of this standard are expressly advised that determination of the validity of any patent rights, and the risk of infringement of such rights, is entirely their own responsibility.

Documents
Document Sharing Hub

Full document details: BS EN IEC/IEEE 63184:2025

IEC/IEEE 63184 was prepared by IEC technical committee 106: Methods for the assessment of electric, magnetic and electromagnetic fields associated with human exposure, in cooperation with International Committee on Electromagnetic Safety (ICES) of the IEEE Standards Association, under the IEC/IEEE Dual Logo Agreement between IEC and IEEE. It is an International Standard.

This document is published as an IEC/IEEE Dual Logo standard.

The text of this International Standard is based on the following IEC documents:

Draft	Report on voting
106/669/FDIS	106/685/RVD

Full information on the voting for its approval can be found in the report on voting indicated in the above table.

The language used for the development of this International Standard is English.

This document was drafted in accordance with the rules given in the ISO/IEC Directives, Part 2, available at www.iec.ch/members_experts/refdocs. The main document types developed by IEC are described in greater detail at www.iec.ch/publications/.

This first edition of IEC/IEEE 63184 cancels and replaces the first edition of IEC PAS 63184 published in 2021. This edition constitutes a technical revision.

This edition includes the following significant technical changes with respect to the previous edition:

a) lower frequency bound changed from 1 kHz to 3 kHz;
b) clarified contact currents as indirect effects in assessment procedures;
c) in measurement methods applied the formulas of SAR and internal electric field;
d) in computational assessment methods added specifications for averaging of current density and internal E-field;
e) updated uncertainty of computational methods;
f) introduced test reporting contents guidance.

The IEC Technical Committee and IEEE Technical Committee have decided that the contents of this document will remain unchanged until the stability date indicated on the IEC website under webstore.iec.ch in the data related to the specific document. At this date, the document will be

- reconfirmed,
- withdrawn, or
- revised.

Documents
Document Sharing Hub

Full document details: BS EN IEC/IEEE 63184:2025

INTRODUCTION

The wireless power transmission systems described in the scope of this document require particularly developed procedures and protocols for the assessment of human exposure. Such systems are increasingly being implemented in a wide range of applications at different frequency ranges from consumer electronics (e.g. mobile phones, tablet PCs) to automotive (electric vehicles). Human exposure to electric and magnetic fields is limited to avoid established adverse health effects, including electrostimulation of nervous tissues and thermal effects, as well as contact currents. A published ITU-R report (ITU-R SM.2303-3 [1][1]) on WPT systems specifies RF exposure assessment methodologies, yet no definitive assessment method was introduced. An exposure assessment method of WPT for EV charging systems was specified in IEC 61980-3:2022 [2]; however, there are currently no other detailed product standards related to WPT systems. Because WPT systems will continue to become ubiquitous in a multitude of applications in the future, IEC and IEEE established a joint working group to address WPT system assessment methods related to human exposures to electric, magnetic, and electromagnetic fields.

In this document, the basic methods to assess both direct and indirect effects of exposure to WPT systems, case studies, and relevant research are specified. These methods mainly focus on frequencies between 3 kHz and 30 MHz and consider both electrostimulation and thermal effects. Future editions will consider extended guidance for assessments of exposure from capacitive WPT systems.

[1] Numbers in square brackets refer to the Bibliography.

Documents
Document Sharing Hub

Full document details: BS EN IEC/IEEE 63184:2025

ASSESSMENT METHODS OF THE HUMAN EXPOSURE TO ELECTRIC AND MAGNETIC FIELDS FROM WIRELESS POWER TRANSFER SYSTEMS – MODELS, INSTRUMENTATION, MEASUREMENT AND COMPUTATIONAL METHODS AND PROCEDURES (FREQUENCY RANGE OF 3 kHz TO 30 MHz)

1 Scope

The objective of this document is to specify methods to assess human exposure to electromagnetic fields generated by stationary wireless power transfer (WPT) in terms of specific absorption rate (SAR), internal electric fields[2] or current density, and contact currents. The frequency range covered by this document is from 3 kHz to 30 MHz. This document focuses on exposures from inductive WPT systems and specifies:

- general compliance assessment procedures;
- measurement methods;
- computational assessment methods;
- assessment combining measurement and computational methods.

This document does not consider the immunity of cardiac implantable electrical devices to radiated disturbances from WPT systems.

2 Normative references

The following documents are referred to in the text in such a way that some or all of their content constitutes requirements of this document. For dated references, only the edition cited applies. For undated references, the latest edition of the referenced document (including any amendments) applies.

IEC 61786-1:2013, *Measurement of DC magnetic, AC magnetic and AC electric fields from 1 Hz to 100 kHz with regard to exposure of human beings – Part 1: Requirements for measuring instruments*
IEC 61786-1:2013/AMD1:2024

IEC 61786-2:2014, *Measurement of DC magnetic, AC magnetic and AC electric fields from 1 Hz to 100 kHz with regard to exposure of human beings – Part 2: Basic standard for measurements*

IEC/IEEE 62209-1528:2020, *Measurement procedure for the assessment of specific absorption rate of human exposure to radio frequency fields from hand-held and body-mounted wireless communication devices – Part 1528: Human models, instrumentation, and procedures (Frequency range of 4 MHz to 10 GHz)*

IEC/IEEE 62704-1:2017, *Determining the peak spatial-average specific absorption rate (SAR) in the human body from wireless communications devices, 30 MHz to 6 GHz – Part 1: General requirements for using the finite difference time-domain (FDTD) method for SAR calculations*

[2] Internal electric field is associated with exposure assessments of nerve stimulation effects; further information is available in e.g. [5].

AVA Documents
Document Sharing Hub

IEC/IEEE 62704-4:2020, *Determining the peak spatial-average specific absorption rate (SAR) in the human body from wireless communications devices, 30 MHz to 6 GHz – Part 4: General requirements for using the finite element method for SAR calculations*

3 Terms and definitions

For the purposes of this document, the following terms and definitions apply.

ISO, IEC, and IEEE maintain terminology databases for use in standardization at the following addresses:

- IEC Electropedia: available at https://www.electropedia.org/
- ISO Online browsing platform: available at https://www.iso.org/obp
- IEEE Dictionary Online: available at http://dictionary.ieee.org

3.1
exposure
<of a body> situation that occurs wherever a person is subjected to electric, magnetic, or electromagnetic fields

3.2
basic restriction
BR
maximum permissible field level induced in the body of a person exposed to electric, magnetic or electromagnetic fields below which established adverse health effects are assumed not to occur

Note 1 to entry: Examples of basic restrictions can be found in International Commission on Non-Ionizing Radiation Protection (ICNIRP) Guidelines [3], [4], [5] and in Annex II of the European Union (EU) Council Recommendation 1999/519/EC [6].

Note 2 to entry: Documents issued by the IEEE ICES TC 95, such as [7] and [8], refer to the basic restrictions as dosimetric reference limits (DRL).

Note 3 to entry: European Union (EU) Directive 2013/35/EU [9] refers to basic restrictions as "exposure limit values" (ELVs), i.e. "values established on the basis of biophysical and biological considerations, in particular on the basis of scientifically well-established short-term and acute direct effects, i.e. thermal effects and electrical stimulation of tissues."

3.3
reference level
maximum permissible level of the incident electric, magnetic, or electromagnetic fields below which the basic restrictions are assumed not to be exceeded

Note 1 to entry: Examples of reference levels can be found in ICNIRP Guidelines [3], [4], [5] and in Annex II of the European Union (EU) Council Recommendation 1999/519/EC [6].

Note 2 to entry: Documents issued by the IEEE ICES TC 95, such as [7] and [8], refer to the reference levels as exposure reference levels (ERL).

Note 3 to entry: European Union (EU) Directive 2013/35/EU [9] refers to reference levels as "action levels (ALs)," i.e. "operational levels established for the purpose of simplifying the process of demonstrating the compliance with relevant ELVs or, where appropriate, to take relevant protection or prevention measures specified in this Directive."

3.4
direct effect
biological effect resulting from exposure of the body to electric, magnetic, or electromagnetic fields without interaction with a conducting object

Documents
Document Sharing Hub

Full document details: BS EN IEC/IEEE 63184:2025

3.5
indirect effect
effect caused by the presence of an object or a substance in an electromagnetic field, which might present a safety or health hazard

3.6
incident field
field that corresponds to the field that would have been present in the absence of an exposed person or phantom

Note 1 to entry: In some documents, the incident field is called an unperturbed field or environmental field.

3.7
coupling factor
factor to conservatively convert an incident field level into an induced field level

Note 1 to entry: Generally, coupling factors are determined by evaluating the correlation between incident and induced fields for a large number of exposure configurations.

3.8
coverage factor
factor that is applied in a physical relation to conservatively compensate for effects that are not considered in the formulation of the relation itself and would lead to an overly complicated formulation if evaluated accurately

3.9
electric field strength
vector field quantity $\boldsymbol{E}$ which exerts on any charged particle at rest a force $\boldsymbol{F}$ equal to the product of $\boldsymbol{E}$ and the electric charge Q of the particle:

$$\boldsymbol{F} = Q\,\boldsymbol{E}$$

[SOURCE: IEC 60050-121:1998 [10], 121-11-18]

3.10
internal electric field
$\boldsymbol{E}_{\mathbf{ind}}$
<in a body> internal electric field induced inside the body as a result of exposure to electric, magnetic, or electromagnetic fields

3.11
peak internal electric field
$p\boldsymbol{E}_{\mathbf{ind}}$
peak instantaneous internal electric field induced inside the body as a result of exposure to electric, magnetic, or electromagnetic fields that is the maximum local, maximum cube averaged (cube length 2 mm) E-field or maximum line averaged (5 mm) E-field

3.12
peak instantaneous internal electric field
$p\boldsymbol{E}_{\mathbf{ind,inst}}$
maximum internal electric field in time-domain for modulated signals calculated by the multiplication of pE_{ind} with the square root of the peak-to-average ratio

3.13
magnetic field strength
vector quantity obtained at a given point by subtracting the magnetization $\boldsymbol{M}$ from the magnetic flux density $\boldsymbol{B}$ divided by the magnetic constant μ_0

Documents
Document Sharing Hub
Full document details: BS EN IEC/IEEE 63184:2025

[SOURCE: IEC 60050-121:1998 [10], 121-11-56, modified – The symbol, formula and Notes to entry have been deleted.]

3.14
magnetic flux density
vector field quantity $\boldsymbol{B}$ which exerts on any charged particle having velocity $\boldsymbol{v}$ a force $\boldsymbol{F}$ equal to the product of the vector product $\boldsymbol{v} \times \boldsymbol{B}$ and the electric charge Q of the particle:

$$\boldsymbol{F} = Q\boldsymbol{v} \times \boldsymbol{B}$$

Note 1 to entry: The divergence of $\boldsymbol{B}$ is zero at all points:

$$\text{div}\,\boldsymbol{B} = 0$$

Note 2 to entry: The magnetic flux density $\boldsymbol{B}$ is sometimes called magnetic field, risking confusion with the magnetic field strength $\boldsymbol{H}$.

[SOURCE: IEC 60050-121:1998 [10], 121-11-19]

3.15
contact current
<for human body> current flowing between the body and an object at a different electric potential (i.e. when either the body or the object is charged by an EMF)

Note 1 to entry: This is the localized current flow into the body, usually the hand, for a light brushing contact.

[SOURCE: ICNIRP 1998 [4]]

3.16
current density
amount of current per unit cross-section area

Note 1 to entry: Current density is related to the internal electric field by Ohm's Law:

$$\boldsymbol{J} = \sigma \boldsymbol{E}$$

where σ is the electrical conductivity of the medium.

[SOURCE: ICNIRP 1998 [4]]

3.17
specific absorption rate
SAR
measure of the rate at which energy is absorbed by the human body when exposed to a radio frequency electromagnetic field

Note 1 to entry: The SAR in the tissue or tissue-equivalent medium can be determined by the rate of temperature increase or by E-field measurements, according to the following formulas:

$$SAR = c_{\mathrm{h}} \left. \frac{\partial T}{\partial t} \right|_{t=0}$$

$$SAR = \frac{\sigma E^2}{\rho}$$

Documents
Document Sharing Hub
Full document details: BS EN IEC/IEEE 63184:2025

where

SAR is the specific absorption rate in watts per kilogram (W/kg);

E is the RMS value of the electric field strength in the tissue medium in volts per metre (V/m);

σ is the electrical conductivity of the tissue medium in siemens per metre (S/m);

ρ is the mass density of the tissue medium in kilograms per cubic metre (kg/m^3);

c_h is the specific heat capacity of the tissue medium in joules per kilogram per kelvin, J/(kg K);

$\left.\frac{\partial T}{\partial t}\right|_{t=0}$ is the initial time derivative of temperature in the tissue medium in kelvin per second (K/s).

[SOURCE: IEC/IEEE 62209-1528:2020, 3.51]

3.18
peak spatial-average SAR
psSAR
maximum average SAR within a local region based on a specific averaging volume or mass

Note 1 to entry: Typical averaging masses are 1 g or 10 g of tissue.

Note 2 to entry: The shape of the averaging volume is cubic as specified in [3] and [8].

3.19
magnitude
<of a vector> for any vector $\boldsymbol{U}$, non-negative scalar, usually denoted by $|\boldsymbol{U}|$, equal to the non-negative square root of the scalar product or, in the case of a complex vector, of the Hermitian product of the vector by itself

[SOURCE: IEC 60050-102:2008 [11], 102-03-23, modified – The Notes to entry have been deleted.]

3.20
gradient
vector ∇f associated at each point of a given space region with a scalar f, having a direction normal to the surface on which the scalar field has a constant value, in the sense of increasing value of f, and a magnitude equal to the absolute value of the derivative of f with respect to distance in this normal direction

Note 1 to entry: The scalar f can refer to a component of a vector field.

[SOURCE: IEC 60050-102:2008 [11], 102-05-19, modified – Note 1 to entry has been replaced; Notes 2 and 3 to entry have been deleted.]

3.21
phantom
physical model with an equivalent human anatomy and comprised of a tissue-equivalent medium with dielectric properties specified in this document

[SOURCE: IEC/IEEE 62209-1528:2020, 3.39]

Documents
Document Sharing Hub

Full document details: BS EN IEC/IEEE 63184:2025

3.22
complex relative permittivity
<under sinusoidal conditions in a medium> complex quantity $\underline{\varepsilon}_r$ that linearly relates the electric flux density and the electric field strength

$$\underline{\boldsymbol{D}} = \varepsilon_0 \underline{\varepsilon}_r \underline{\boldsymbol{E}}$$

where

$\underline{\boldsymbol{D}}$ is the electric flux density phasor,

$\underline{\boldsymbol{E}}$ is the electric field strength phasor;

ε_0 is the dielectric permittivity of free space

Note 1 to entry: The complex relative permittivity is generally frequency dependent. For an isotropic medium the complex relative permittivity is a scalar; for an anisotropic medium it is a tensor.

Note 2 to entry: Generally $\underline{\varepsilon}_r$ is expressed as $\underline{\varepsilon}_r = \varepsilon_r' - \mathrm{j}\varepsilon_r''$ where ε_r' is the real relative permittivity and ε_r'' is the dielectric loss index. In the context of this document, it represents the conductivity of free charges in the exposed tissue or tissue-equivalent medium $\sigma = \omega\varepsilon_0\varepsilon_r''$.

[SOURCE: IEC 60050-121:2019 [10], 121-12-14, modified – reworded definition for replacing the term in context.]

3.23
device under test
DUT
device that is tested in accordance with the procedures specified in this document

3.24
post-processing
computation of physical quantities based on the reading of the results of a measurement or on the output of computational software

Note 1 to entry: Examples of the computation are the conversion of currents or voltages obtained from a calibrated probe into electric field strength or magnetic field strength or the averaging of field quantities, e.g. the local SAR distribution for assessment of psSAR.

3.25
wireless power transfer
WPT
transmission of electrical energy by electric, magnetic, or electromagnetic fields without wire or cable connection between the energy source and the load for wireless charging

Documents
Document Sharing Hub
Full document details: BS EN IEC/IEEE 63184:2025

4 Symbols and abbreviated terms

4.1 Physical quantities

The internationally accepted SI units are used throughout this document.

Symbol	Quantity	Unit	Dimensions
B	Magnetic flux density	tesla	T
c_h	Specific heat capacity	joule per kilogram per kelvin	J/(kg K)
E	Electric field strength	volt per metre	V/m
f	Frequency	hertz	Hz
H	Magnetic field strength	ampere per metre	A/m
J	Current density	ampere per square metre	A/m^2
P	Average (temporal) absorbed power	watt	W
T	Temperature	kelvin	K
ε	Permittivity	farad per metre	F/m
λ	Wavelength	metre	m
σ	Electric conductivity	siemens per metre	S/m

NOTE In this document temperature is quantified in degrees Celsius, as defined by: T (°C) = T (K) − 273,15 K.

4.2 Constants

Symbol	Physical constant	Magnitude
η_0	Intrinsic impedance of free space	120π Ω or 377 Ω
ε_0	Permittivity of free space	$8{,}854 \times 10^{-12}$ F/m
μ_0	Permeability of free space	$4\pi \times 10^{-7}$ H/m
j	Imaginary unit	1

4.3 Abbreviated terms

BEM boundary element method
B-field magnetic flux density
BR basic restriction
DRL dosimetric reference limit
DUT device under test
E-field electric field strength
ERL exposure reference level
EV electric vehicle
FDFD finite difference frequency domain
FDTD finite difference time domain
FEM finite element method
FIT finite integration technique
GGSM generic gradient source model
H-field magnetic field strength
IM impedance method
MFS magnetic field source

Documents
Document Sharing Hub

MQS	magneto-quasi-static
MoM	method of moments
psSAR	peak spatial-average SAR
pE_{ind}	peak instantaneous internal electrical field
RF	radio frequency
RL	reference level
RMS	root mean square
RPA	remotely piloted aircraft
RSS	root sum square
SAR	specific absorption rate
SPFD	scalar potential finite difference
WPT	wireless power transfer (system)

5 Assessment procedures

5.1 General

Compliance assessment is to be carried out in terms of specific absorption rate (SAR), internal electric fields, or current density; and contact currents. Figure 1 presents a flowchart for the assessment procedure for evaluating both the direct effects (internal electric field, current density, or SAR) and contact currents of electromagnetic fields generated by WPT systems. The assessment methods for these quantities are different.

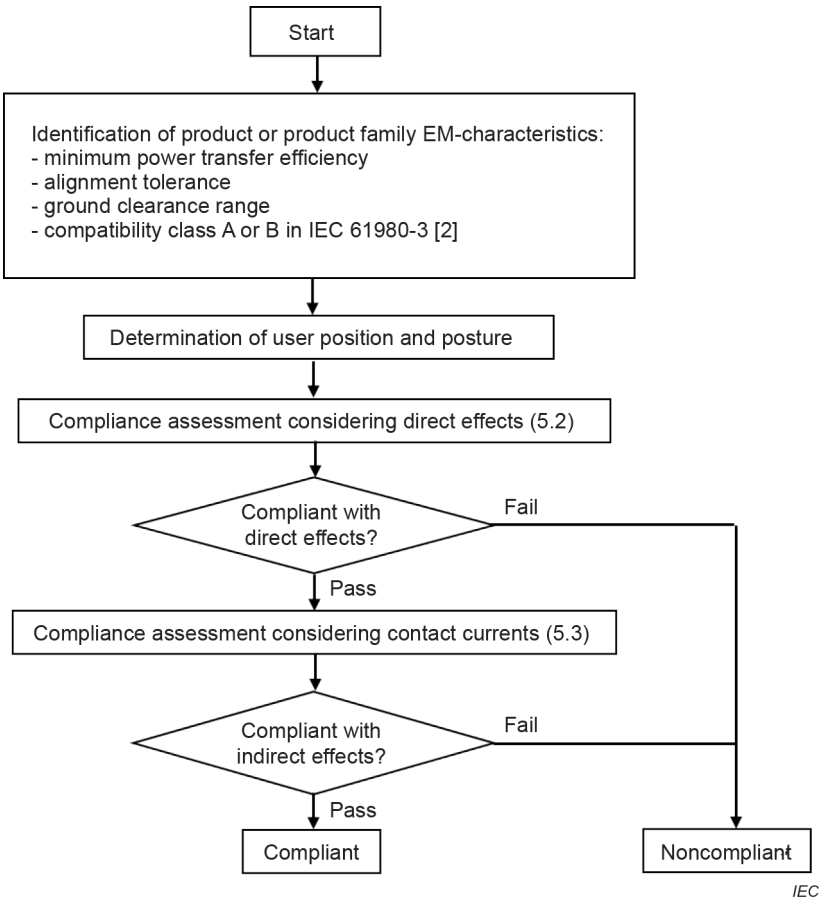

Figure 1 – Flowchart for the assessment procedure

Documents
Document Sharing Hub
Full document details: BS EN IEC/IEEE 63184:2025

5.2 Compliance assessment considering direct effects

5.2.1 General

Subclause 5.2 provides basic assessment methods considering the direct effects of electromagnetic fields [3], [4], [5], [8]. Evaluations are made in terms of either the incident fields or of the induced fields according to the averaging methods as specified in [3], [4], [5], [8]. This document specifies the implementation of appropriate averaging techniques (Annex G), and references to documents where these are specified. The following list and Figure 2 specify four tiers to assess exposure from WPT and demonstrate conformity with the basic restrictions or reference levels. Any of the four tiers may be selected. They require increasing technical effort and yield decreasing levels of conservativeness.

a) Tier 1: The evaluation of the exposure based on coil current is straightforward but is the most conservative one (5.2.2). The Tier 1 method does not evaluate the exposure from the incident electric field.

b) Tier 2: Assessment of the incident fields and comparison against reference levels is specified in 5.2.3.

c) Tier 3: The incident magnetic fields can be applied to conservatively evaluate the induced fields for comparison with reference levels or basic restrictions using the gradient-source-based method specified in 5.2.4.

d) Tier 4: Direct evaluation of the fields induced in the body or in a body phantom using measurement or computational methods is specified in 5.2.5.

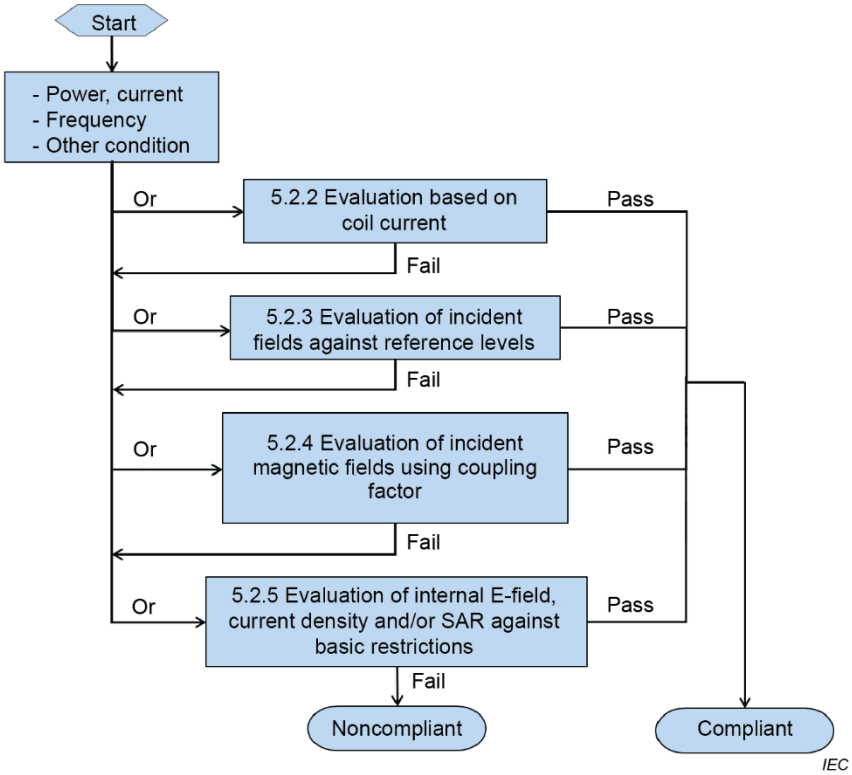

Figure 2 – Flowchart for the assessment procedure considering direct effects

Documents
Document Sharing Hub
Full document details: BS EN IEC/IEEE 63184:2025

5.2.2 Tier 1: Evaluation based on coil current

According to Clause A.1, the maximum permissible coil current I_{mp} can be approximated by evaluating the magnetic flux density of a circular coil at a fixed distance of 10 mm and comparing it against the reference level B_{RL}. For a circular coil with radius r, I_{mp} can be estimated using Formula (1):

$$I_{mp}(r) = \frac{2\pi d_0 B_{RL}}{\mu_0 n} e^{-\frac{r_0}{r}} \quad (1)$$

where

r is the maximum coil radius (or half of the largest dimensions of non-circular coils);

d_0 is the fixed distance of 10 mm at which the magnetic flux density is compared to B_{RL};

B_{RL} is the reference level of magnetic flux density;

μ_0 is the free space permeability, $4\pi \times 10^{-7}$ H/m;

n is the number of turns of the coil;

r_0 is a constant of 21,5 mm.

NOTE The value of r_0 was determined from a curve fit to the numerical solution of the Bio-Savart equation.

The measured coil current shall be less than the calculated I_{mp}.

The approximation of Formula (1) is conservative for fields in the plane of the coil outside its circumference if the diameter of the coil windings is smaller than d_0. It cannot be applied within the circumference of the coil. Above and below the plane of the coil, the fields can be assumed to decay monotonically.

If it cannot be demonstrated that approximation of Formula (1) is conservative for the DUT or the evaluation distance is different from d_0, then results in accordance with 5.2.2 are not valid even if the coil current is lower than the I_{mp}.

Because it can be shown that the B-field decays monotonically as a function of the distance from the coil for any coil radius r, results from Formula (1) can be regarded as conservative for distances from the coil larger than d_0 within the uncertainty of the applied approximation (Clause A.1).

Annex A provides additional information regarding exposure evaluations using approximations.

Documents
Document Sharing Hub

Full document details: BS EN IEC/IEEE 63184:2025

5.2.3 Tier 2: Evaluation of incident fields against reference levels

Both incident electric and magnetic field strengths are assessed at different distances including the closest distance, and in all directions where the DUT can operate near people. The assessment can be carried out using measurement or computational methods or basic calculations.

Depending on the applicable exposure guidelines:

– Above 100 kHz, the incident fields shall be spatially averaged.
– Below 100 kHz, incident fields can be averaged in space over the body or as specified in Annex I.
– Different reference averaging-time periods can be specified for proper assessment of the incident fields against reference levels.

NOTE 1 Additional details on when spatial averaging is permitted can be specified in the exposure guidelines or in national regulations.

NOTE 2 For example, Annex I and Annex J introduce an averaging method for WPT EV systems for persons standing next to the EV on a non-conductive ground. The method is based on the three-point method introduced in [12], which shows that the approach is conservative for measurement distances larger than 20 cm and frequencies up to 100 kHz.

NOTE 3 In some exposure guidelines, the electric and magnetic field strengths are assessed with both an instantaneous (to prevent nerve stimulation) and six minutes reference averaging-time periods.

5.2.4 Tier 3: Evaluation of incident magnetic fields using coupling factor

5.2.4.1 General

The reference levels of electromagnetic fields are derived from the maximum coupling conditions between the fields and the human body, i.e. the maximum induced quantities in the human body exposed to the uniform electromagnetic fields.

Coupling factors for magnetic field exposure can be applied for the incident field to mitigate the over-estimation and still warrant conservativeness with respect to the basic restrictions, based on Formula (2).

$$QoI = k \times F \tag{2}$$

where

QoI is the quantity of interest to be compared in terms of the basic restrictions;

k is a generic coupling factor that shall be derived according to 5.2.4.2 for specific coil configurations and evaluation distances, or according to 5.2.4.3 for the generic gradient source model (GGSM);

F is the measured incident field at the location of the evaluation.

Two methods are specified in this document as options:

- the coupling factor k_L is estimated from localized exposure scenarios as specified in 5.2.4.2;
- the generally applicable coupling factor k_G is characterized with respect to the normalized incident magnetic field gradient at the location of the exposure evaluation by applying the GGSM method [13] (5.2.4.3).

NOTE The method specified in 5.2.4.2 uses coupling factors for the maximum induced current density, electric field, and SAR. The calculation results of coupling factors are listed in IEC TR 62905 [14]. The GGSM method specified in 5.2.4.3 specifies coupling factors for all basic restrictions of [3], [4], [5], and [8].

The methods of 5.2.4.2 or 5.2.4.3 can be applied only under the following conditions:

AVA Documents Document Sharing Hub

a) The induced quantities such as internal electric field, current density, or SAR caused by incident electric fields are negligible compared to those induced by the incident magnetic fields.

b) The whole-body average SAR is negligible compared to the local exposure limits, and the contribution of the psSAR or the internal electric field is dominant.

c) Evaluation conditions such as frequency, field distribution, distance to human body, etc., are identical to those used in the derivation of the coupling factor. Otherwise the uncertainty due to the deviation shall be determined following the methodologies of [12], [15] for 5.2.4.2, and of [13] for 5.2.4.3.

d) Quasi-static conditions (7.2) apply for the incident magnetic field.

In addition to the variables specified for Formula (2), descriptions of the symbols used in the formulas of 5.2.4.2 and 5.2.4.3 are consolidated in Table 1.

Table 1 – List of symbols used in the formulas of 5.2.4.2 and 5.2.4.3

Symbol	Description	Constant	Formula (#)
B_0	is a constant normalization magnetic flux density of 6,25 µT [5]	yes	(14)
B_1	is a constant normalization magnetic flux density of 2,04 µT [16]	yes	(15)
$B_{\text{inc,meas}}$	is the local magnetic flux density measured by a field probe or evaluated computationally	no	(12), (13)
B_{max}	is the maximum magnetic flux density in the absence of a person at a point inside the bounding box within which the person could be located	no	(3), (4), (5)
$B_{\text{max}}(G_n)$	is the maximum measured magnetic flux density at the human body surface when the field gradient is G_n	no	(6)
B_{RL}	is the applicable reference level of the magnetic flux density B or a fixed normalization value, e.g. B_0	yes	(3), (4), (5), (6), (12), (13)
c_3	constant = 1 m^{-1}	yes	(7), (8), (9), (10), (11)
E_{BR}	is the basic restriction of internal electric field strength	yes	(4), (12)
E_{max}	is the maximum internal electric field strength induced in the human body	no	(4)
F	is the measured incident field at the location of the evaluation	no	(2)
f_0	is a constant normalization frequency of 100 kHz	yes	(14), (15)
G_n	normalized local B-field gradient perpendicular to the skin surface of the exposed body	no	(6), (7), (8), (9), (10), (11)
$G_{n,\text{meas}}$	measured normalized local B-field gradient	no	(12), (13), (14), (15)
J_{BR}	is the basic restriction of current density	yes	(3), (13)
J_{max}	is the maximum current density induced in the human body	no	(3)
k	is a generic coupling factor that shall be derived according to 5.2.4.2 for specific coil configurations and evaluation distances, or according to 5.2.4.3 for the generic gradient source model (GGSM)	yes	(2)
$k(G_{n,\text{meas}})$	is the value of the coupling factor calculated for the specific gradient $G_{n,\text{meas}}$	yes	(12), (13)
$k_{B,\text{10g}}$	is the low frequency magnetic flux density coupling coefficient for psSAR10g, 2 × 10^{-4}	yes	(14)
$k_{B,\text{1g}}$	is the low frequency magnetic flux density coupling coefficient for psSAR1g, 4,6 × 10^{-5}	yes	(15)
$k_{\text{G},E;\ \text{line}}$	coupling factor for induced E-field averaged over a line of 5 mm	yes	(8)
$k_{\text{G},e;\ \text{cube}}$	coupling factor for induced E-field averaged over a cube of 8 mm^3	yes	(7)

AVA Documents
Document Sharing Hub

Symbol	Description	Constant	Formula (#)
$k_{\mathrm{G},e;\ \mathrm{circle}}$	coupling factor for current density averaged over an area of 1 cm^2	yes	(9)
$k_{\mathrm{G,psSAR10g}}$	coupling factor for peak spatial SAR averaged over a cube of 10 g	yes	(10), (14)
$k_{\mathrm{G,psSAR1g}}$	coupling factor for peak spatial SAR averaged over a cube of 1 g	yes	(11), (15)
QoI	is the quantity of interest to be compared to the basic restrictions	no	(2)
QoI_{BR}	is the basic restriction of the induced metric QoI	yes	(6)
$QoI_{\mathrm{max}}(G_n)$	represents the maximum of the induced quantity of interest (electric field strength, current density, or SAR) in the body when the field gradient is G_n	no	(6)
SAR_{BR}	is the basic restriction for psSAR	yes	(5), (14), (15)
SAR_{max}	is the maximum psSAR induced in the human body	no	(5)

5.2.4.2 Coupling factor k_{L} based on the analysis of localized exposure scenarios

The coupling factor for the current density $k_{\mathrm{L},J}$ is determined using Formula (3).

$$k_{\mathrm{L},J} = \frac{J_{\mathrm{max}} / B_{\mathrm{max}}}{J_{\mathrm{BR}} / B_{\mathrm{RL}}} \tag{3}$$

where the symbols are specified in Table 1 of 5.2.4.1.

NOTE 1 The coupling factor was originally introduced for exposure assessments in low frequencies in IEC TR 62905:2018 [14], IEC 62226-2-1 [17] and IEC 62311:2007 [18], then amended in IEC 62233 [19].

Using this coupling factor, the measured magnetic field strength, multiplied by the coupling factor, is directly compared to the reference level.

The concept of exposure assessment using coupling factor is expanded to the internal electric field and SAR with Formula (4) and Formula (5) ([12], [15]).

$$k_{\mathrm{L},E} = \frac{E_{\mathrm{max}} / B_{\mathrm{max}}}{E_{\mathrm{BR}} / B_{\mathrm{RL}}} \tag{4}$$

$$k_{\mathrm{L},SAR} = \frac{\sqrt{SAR_{\mathrm{max}}} / B_{\mathrm{max}}}{\sqrt{SAR_{\mathrm{BR}}} / B_{\mathrm{RL}}} \tag{5}$$

where the symbols are specified in Table 1 of 5.2.4.1.

E_{BR} and B_{RL} depend on frequency. The coupling factor k_{L} is multiplied by the measured magnetic fields to consider the effects of field non-uniformity. Conservative coupling factors k_{L} are typically determined by simulation with the ratio of the induced quantities to the incident magnetic field ([12], [15]), e.g. for a specific frequency, field distribution, distance to human body and for different anatomies. Based on such an evaluation, conservative values of the coupling factors can be derived, the uncertainty of which shall be estimated and documented following the methodology applied in [12], [15]. Appropriate methods for the computational modelling of the coil and the exposed person are specified in Clause 7.

AVA Documents
Document Sharing Hub
Full document details: BS EN IEC/IEEE 63184:2025

NOTE 2 See also Annex F and Annex G. Annex H specifies procedures for validation of the computational results.

Exposure in terms of the internal electric field strength, current density, or psSAR is then assessed by comparing the multiplied value to the reference level of the magnetic fields only.

5.2.4.3 Coupling factor k_G based on the GGSM method

A generally applicable coupling factor $k_G(G_n)$ is introduced using the GGSM of [13] to mitigate over-estimation by incident magnetic field assessment in strong field gradients that are common in the vicinity of WPT systems. The method is conservative for real sources because the coupling factors are derived from a 2D gradient model, whereas real sources have gradients in 3D. However, it requires evaluation of both the local field amplitude and the local gradient in the normal direction with respect to the exposed body, as indicated in Figure 3.

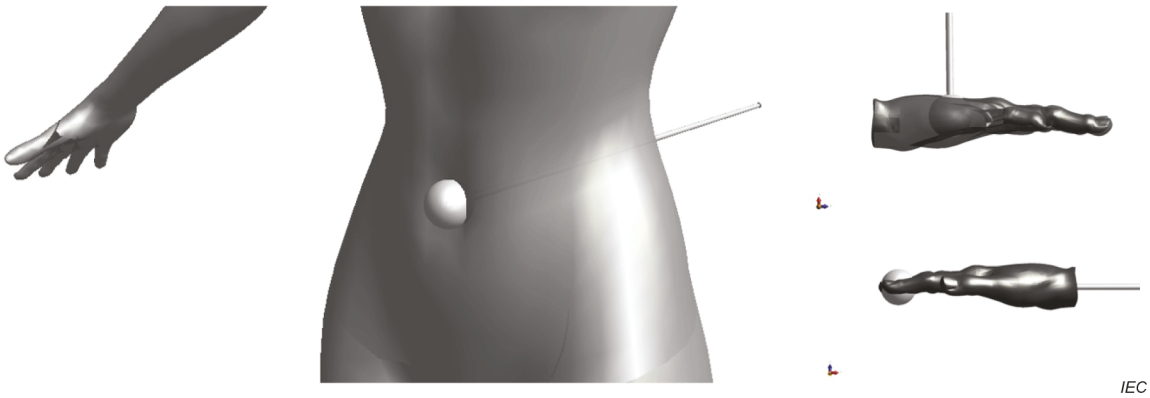

NOTE In each view the sphere with attached shaft symbolizes example locations of a field probe to measure the field amplitude for evaluating the gradient at the reference location (body surface).

Figure 3 – The gradient G_n is determined at the surface and normal to the surface, i.e. in the direction of the axis shown

The method applies the following quantities of the incident magnetic field at the location of the exposed body:

– frequency;
– magnetic flux density (B_{xyz}) at the skin surface of the exposed body;
– normalized local B-field gradient G_n (T/m/T) perpendicular to the skin surface of the exposed body.

NOTE 1 Because the coupling factors only depend on the spatial properties of the incident magnetic field and not on its amplitude, they are given for the field gradient normalized to the local field amplitude and expressed in units of T/m/T.

Documents
Document Sharing Hub
Full document details: BS EN IEC/IEEE 63184:2025

The GGSM coupling factors have been determined for a wide range of 2D gradients (i.e. uniform in one direction) from a generic magnetic field source comprised of two parallel line currents with equal amplitudes but 180° phase difference and different separation distances as specified in [13]. This source has a magnetic flux density B and a normalized B-field gradient G_n that depend on a position relative to the GGSM source and the magnitude of the source current. The fields induced in the exposed body are normalized to the maximum B-field amplitude and normalized B-field gradient at the skin surface. Based on a large-scale computational study including human body models of different ages, heights, and weights [13], worst-case exposure conditions (i.e. the highest induced field quantities) were determined for each normalized B-field gradient and frequency analysed. The coupling factors $k_{\mathrm{G}}(G_n)$ are determined using Formula (6):

$$k_{\mathrm{G},QoI} = \frac{QoI_{\mathrm{max}}(G_n)/B_{\mathrm{max}}(G_n)}{QoI_{\mathrm{BR}}/B_{\mathrm{RL}}} \tag{6}$$

where the symbols are specified in Table 1 of 5.2.4.1.

NOTE 2 The coupling factors were determined for the heterogeneous models of the Virtual Population (ViP) ([20], [21]) and can be regarded as conservative, i.e. they already include the enhancement factors caused by tissue boundaries.

The coupling factors of each specific induced metric specified in Annex G according to the guidelines, i.e. [3], [4], and [5], are expressed by physics-based approximations as functions of the gradient of the magnetic flux density, i.e. Formula (7), Formula (8), Formula (9), Formula (10), and Formula (11):

$$k_{\mathrm{G},E;\,\mathrm{cube}}(G_n) = \frac{1}{\left[1 + 6{,}5 \times 10^{-6} \times (G_n/c_3)^{5{,}8}\right]^{(1/5{,}8)}} \tag{7}$$

$$k_{\mathrm{G},E;\,\mathrm{line}}(G_n) = \frac{1}{\left[1 + 4 \times 10^{-11} \times (G_n/c_3)^{6{,}6}\right]^{(1/6{,}6)}} \tag{8}$$

$$k_{\mathrm{G},J;\,\mathrm{circle}}(G_n) = \frac{1}{\left[1 + 4 \times 10^{-3} \times (G_n/c_3)^{2{,}9}\right]^{(1/2{,}9)}} \tag{9}$$

$$k_{\mathrm{G,psSAR\,10\,g}}(G_n) = \left(\frac{1}{\left[1 + 2 \times 10^{-1} \times (G_n/c_3)^{1{,}2}\right]^{(1/1{,}2)}}\right)^2 \tag{10}$$

$$k_{\mathrm{G,psSAR\,1\,g}}(G_n) = \left(\frac{1}{\left[1 + 2{,}5 \times 10^{-1} \times (G_n/c_3)^{1{,}1}\right]^{(1/1{,}1)}}\right)^2 \tag{11}$$

Documents
Document Sharing Hub
Full document details: BS EN IEC/IEEE 63184:2025

where the symbols are specified in Table 1 of 5.2.4.1.

The trend of the approximation formulas as a function of the gradient is shown in Figure 4. The method has been analytically verified (see Appendix of [13]). For any other specific induced metrics or basic restrictions, the process specified in [13] shall be repeated.

To assess exposure in terms of the basic restrictions, the magnetic flux density (B_{meas}) and the normalized field gradient ($G_{n,\text{meas}}$) of the DUT are evaluated at any closest accessible location from the source using equipment that provides both values, or that measures the field using a magnetic vector-field meter at separate locations and derives the gradient vectors of the vector field components of the magnetic field. Here the measured magnetic field gradient is determined at the reference location according to Figure 3.

The internal electric field, current density and SAR can then be predicted by Formula (12), Formula (13), Formula (14), and Formula (15) [13]:

$$E = k_{\text{G},E}\left(G_{n,\text{meas}}\right) \times E_{\text{BR}} \times \frac{B_{\text{inc,meas}}}{B_{\text{RL}}} \tag{12}$$

$$J = k_{\text{G},J}\left(G_{n,\text{meas}}\right) \times J_{\text{BR}} \times \frac{B_{\text{inc,meas}}}{B_{\text{RL}}} \tag{13}$$

$$psSAR_{\text{10g}} = k_{\text{G,psSAR10g}}\left(G_{n,\text{meas}}\right) \times SAR_{\text{BR}} \times \left(\frac{B_{\text{inc,meas}}}{B_0}\right)^2 \times \left(\frac{f}{f_0}\right)^2 \times k_{B,\text{10g}} \tag{14}$$

$$psSAR_{\text{1g}} = k_{\text{G,psSAR1g}}\left(G_{n,\text{meas}}\right) \times SAR_{\text{BR}} \times \left(\frac{B_{\text{inc,meas}}}{B_1}\right)^2 \times \left(\frac{f}{f_0}\right)^2 \times k_{B,\text{1g}} \tag{15}$$

where the symbols are specified in Table 1 of 5.2.4.1.

The formulas presented in this 5.2.4.3, together with Figure 4, quantify the reduction of the induced field quantities in the presence of a magnetic gradient field with a coupling factor k of less than 1.

NOTE 3 An example is a case of two magnetic field sources that operate at an identical frequency and whose magnetic fields at the measurement point are equal. One of them has a uniform magnetic field distribution (G_n = 0), and the magnetic field gradient of the other one is different from zero (the magnetic field decreases in the direction of the human body). In both cases, E_{BR}, B_{RL}, and $B_{\text{inc,meas}}$ are the same, but $k_{G,E}$ = 1 for the uniform field and $k_{G,E}$ < 1 for the field with gradient. This makes the induced electric field E of the non-zero-gradient smaller than that of the no-gradient case.

NOTE 4 For large field gradients, results of Formula (7) through Formula (11) approach zero. This can be explained as that the fields inside the volume of the body being exposed approach zero as the gradient approaches infinity.

The method may be applied using the following steps:

a) determine the incident B-field at all locations at which a body can be exposed to the field of the source and determine the lowest gradient that is normal to the surface of the body (see Figure 3);

b) compute the maximum induced fields according to Formula (12), Formula (13), Formula (14), and Formula (15) for all locations.

AVA Documents
Document Sharing Hub

If the maximum induced field is lower than the applicable basic restriction, the source is compliant.

For the application of this method the conditions listed in 5.2.4.1 shall apply. An additional condition is that the incident magnetic field is dominated by a single source. For conditions different from these, the uncertainty should be determined following the methodology of [13].

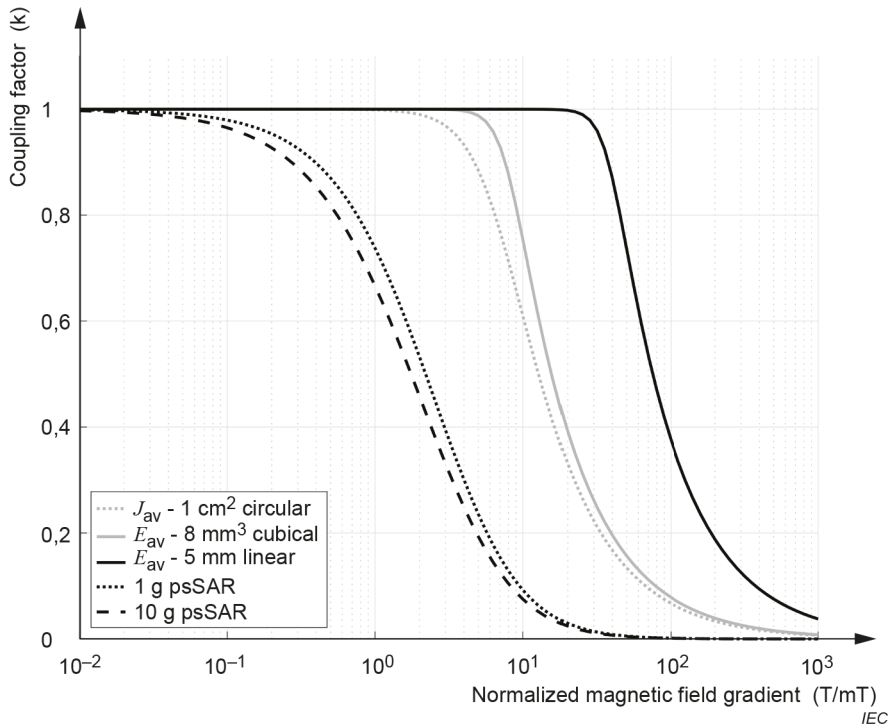

Figure 4 – Coupling factors k of Formula (7) through Formula (11) as a function of the normalized magnetic field gradient [13]

5.2.5 Tier 4: Evaluation of internal E-field, current density, or SAR against basic restrictions

SAR can be measured using a small probe in a liquid-filled phantom which is exposed to the electromagnetic fields of the DUT. The measured values can be directly compared with basic restrictions. The evaluation and validation procedures are specified in IEC/IEEE 62209-1528. The assessment method is specified in detail in 6.2.

NOTE The frequency range of IEC/IEEE 62209-1528:2020 is from 4 MHz to 10 GHz.

Internal electric field, current density, or SAR may be evaluated analytically or by simulation using anatomical models of the human body or models of laboratory phantoms for comparison with basic restrictions. The simulation model and methodology shall be validated as part of the evaluation process. The validation procedure and results shall be documented. The assessment method based on simulation is specified in detail in Clause 7.

5.3 Exposure assessment of contact currents

Contact currents are the only indirect effects considered in this document. They flow into a biological body via a physical contact with the electrode or other source of current.

Contact currents can be assessed either by direct measurement or by measurement of the incident electromagnetic fields.

Documents
Document Sharing Hub
Full document details: BS EN IEC/IEEE 63184:2025

The following considerations shall be applied to assess exposure by incident electromagnetic fields.

– The objects exposed to H-fields are grounded (Figure 5).
– The contact currents as a function of the incident magnetic field strength are calculated with Formula (16), which is derived from Faraday's law.

$$I_c = H_{inc} \frac{2\pi f \mu_0 S}{Z} \tag{16}$$

where

I_c is contact current (RMS);

H_{inc} is the RMS of the incident H-field;

f is the frequency of the incident H-field;

μ_0 is the permeability of free space;

Z is the impedance of the human body (see 6.3);

S is the area of the loop such as 1,5 m × 0,5 m.

Contact currents may be calculated with Formula (16) or measured directly as specified in 6.3. Contact currents can be measured directly using a contact current meter with an ungrounded or grounded metal object placed in the vicinity of the DUT. Figure 5 shows exposure situations for ungrounded and grounded metal objects.

Figure 6 presents a flowchart for the assessment procedure. Details of measurement conditions, measurement setup, etc., are summarized in IEC TR 63167 [22]. The assessment method is specified in detail in 6.3.

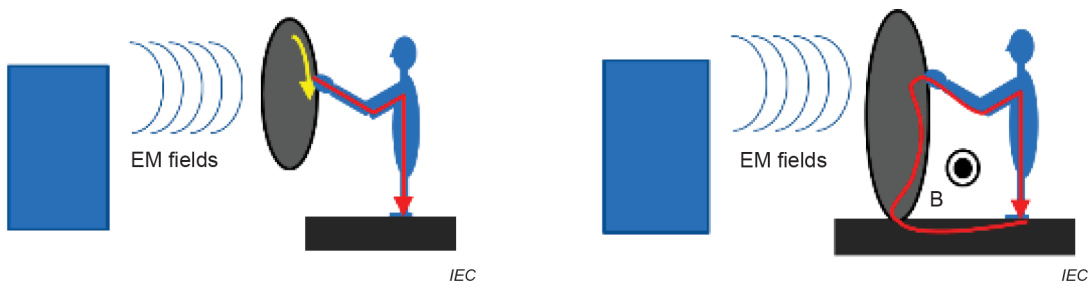

a) Currents when touching ungrounded metal **b) Currents when touching grounded metal**

Figure 5 – Two exposure situations for ungrounded and grounded metal objects

Documents
Document Sharing Hub
Full document details: BS EN IEC/IEEE 63184:2025

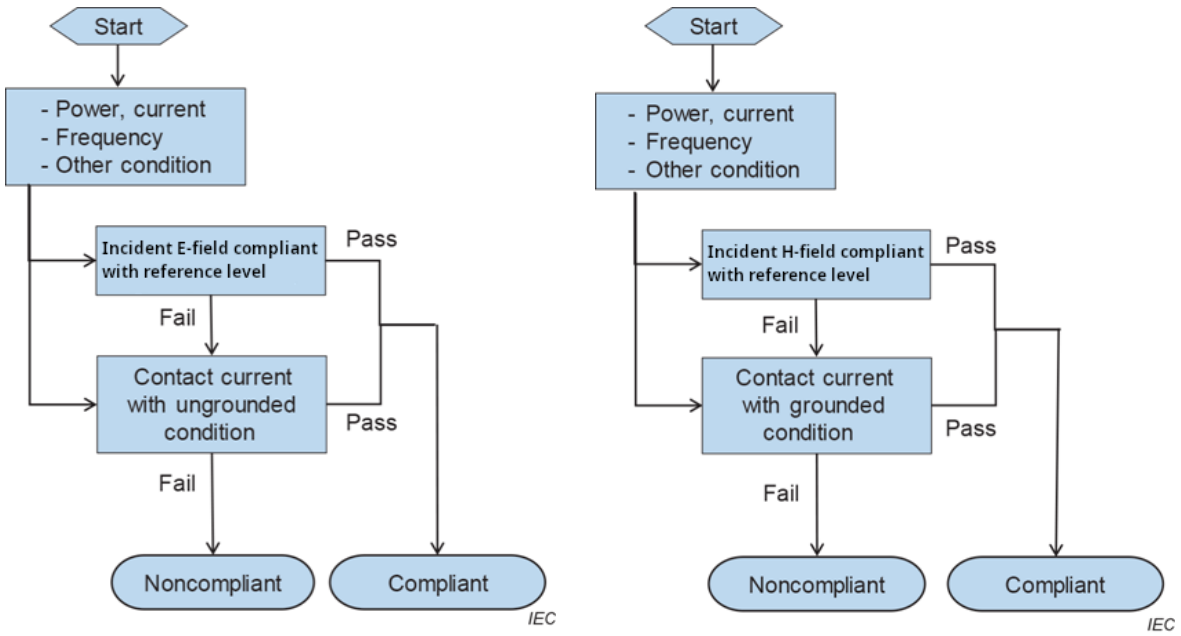

a) ungrounded condition (incident E-field) **b) grounded condition (incident H-field)**

Figure 6 – Flowchart for assessment procedures for contact currents

6 Measurement methods

6.1 Incident fields

6.1.1 General

IEC 61786-1:2013 and IEC 61786-1:2013/AMD1:2024 and IEC 61786-2:2014 specify electromagnetic field basics, measurement methods, and requirements of the measurement equipment at frequencies below 100 kHz. In addition, IEC 62233 [19] and IEC 62311 [18], [23] specify electromagnetic field measurements for the purpose of exposure assessment. This document specifies the requirements for measurement equipment for electromagnetic fields from 3 kHz to 30 MHz.

a) Equipment for measuring electric fields, magnetic fields, and magnetic field gradient is specified in 6.1.2.1, 6.1.2.2, and 6.1.2.3, respectively. The calibration methods are specified in Annex B.

b) The validation method is specified in Annex C.

c) Both incident electric and magnetic field vectors are measured at a specific distance, including the closest distance where the DUT may operate near people. These International Standards specify measurement positions based on the size and regular usage of equipment. IEC 62311 [18], [23] specifies it as a "user's usual position." IEC 62233 [19] specifies the measurement position in detail for household appliances and similar apparatus, including inductive battery chargers.

d) The measured value may be based on either a time-averaged or the maximum instantaneous value of the target electromagnetic field, depending on the characteristics of the source and the exposure metric being assessed.

e) The incident fields are measured in free space without the presence of an exposed body or phantom. The closest measurement distance should be chosen within the range that is accessible to the user.

Documents
Document Sharing Hub
Full document details: BS EN IEC/IEEE 63184:2025

f) When the measurement probe comes close to the source and metallic or highly insulated objects, electromagnetic coupling may occur and the probe sensor impedance changes. Due to the finite size of the probe, all field measurements are subject to some amount of spatial averaging. For a loop, the measurement location may be specified as the geometric centre of the loop, but the result will be a function of the average H-field passing through the loop area. The probe sensor should be sufficiently small for improved accuracy of the measurement of the spatial peak of a given field component. Larger probes are prone to larger uncertainties in strong gradient fields. The gradient and isotropy uncertainty shall be properly evaluated with its instrumentation by simulations and by rotating the probe in the gradient field (9.2.7).

NOTE 1 For example, if an isotropic sensor with a loop area of 1 cm^2 is rotated in a magnetic field with a normalized gradient of 50 T/m/T, which is constant over the area of the loop, the resulting error is less than 1,3 % (rectangular distribution). For a sensor with a loop area of 3 cm^2, it is less than 5 %.

NOTE 2 Additional guidance on incident field measurement configurations, probe size considerations, etc. is available for example in [24].

g) In the case of non-uniform incident fields, the measured field values may be spatially averaged over the exposed regions of the body, with the important provision that the basic restrictions on psSAR and induced electric fields are not exceeded. If averaging is applied in the case where one or more of the measured values are above the reference levels, evidence shall be provided that the assessment based on the averaged values does not lead to exceeding the underlying basic restrictions.

NOTE 3 National regulations can differ from the preceding conditions and pose different requirements, e.g. on frequency range, minimum distance, or acceptability of spatial averaging as specified in step g). Incident electric and magnetic field strengths are measured or calculated in accordance with the applicable regulations.

Assessment procedures for WPT, heavy duty EVs, and remotely piloted aircraft are specified in Clause I.1, Clause I.2, and Clause I.3, respectively. Examples of assessment results are provided in Annex J.

If the incident field consists of multiple frequency components (i.e. above the noise floor of the measurement set-up), these contributions shall be considered in the exposure assessment. Summation regimes (schemes) in Annex A of IEC 62311:2019 [23] may be applied to consider spectral contributions.

6.1.2 Equipment

6.1.2.1 Equipment for electric field strength measurements

Electric field strength can be measured with a calibrated antenna or probe that is sensitive to electric fields exclusively (e.g. small dipoles) and connected to the calibrated measurement equipment.

Two types of antennas or probes are used for electric field measurements: single-axis-sensor types, and three-axis-sensor types in which three sensors are arranged perpendicular to each other. IEC 61786-2 recommends using the three-axis type. Using single-axis instruments is possible in some cases, e.g. when the direction of the field is already known (IEC 61786-1) or if the probe is rotated and all three vector components of the field are evaluated. The electric field strength of the three-axis component readings given in Formula (17) applies:

$$E_{\mathrm{R}} = \sqrt{E_x^2 + E_y^2 + E_z^2} \tag{17}$$

where E_x, E_y, and E_z are effective electric field strengths for the three orthogonal axes.

Three-axis electric field measurement equipment has the advantage of measuring the net field E_{R} regardless of the probe orientation.

Documents
Document Sharing Hub

In general, measurement equipment for electric field strength is either broadband or narrowband. For both measurement systems, the equipment consists of an antenna or probe (including power source), measurement part, and data recording and processing unit. The following describes the system characteristics and selection method.

a) A broadband system uses dipole antennas. It is small enough to improve the uniformity of the sensitivity at each frequency. To improve isotropy, three antennas are generally placed orthogonal to one another and each signal or the combined signal is extracted. This type of antenna is suitable for near-field electromagnetic fields of complicated distributions. A broadband isotropic electric field strength meter designed for radio wave protection is typically used for measurement provided that the electric field strength is uniform over the volume of the probe. Field uniformity can be established by checking that the result remains within the expected measurement uncertainty when the probe is rotated to arbitrary orientations. If the electric field is not sufficiently uniform over the volume of the probe at the measurement location, the uncertainty of the measured field at the centre of the probe caused by the electric field gradient shall be assessed. Other systems may include waveform observation equipment, such as diode detectors and oscilloscopes.

b) A narrowband system is tuned to each target frequency. The measurement system generally has broad measurement frequencies, high receiving sensitivity, and short responses. It is thus also suitable for pulsed waves or multiple sources. However, for the pulsed wave measurement, it is acceptable to measure in the frequency domain where the target frequency range is broader than the passband width of the measurement system. A biconical antenna with broadband characteristics is often used for far-field region because the size of the antenna is not electrically small. A three-axis orthogonal small dipole is suitable for near-field measurements.

c) For an electromagnetic environmental assessment, a broadband isotropic electric field strength meter is preferred unless the DUT cannot be measured properly with such a device, in which case it shall be replaced by another measurement system.

d) The incident E-fields are only measured with low uncertainty if the E-field is uniform or has a constant gradient over the entire E-field sensor. Only these types of field sources are relevant for human exposure. Localized E-field sources caused by accumulation of charges have a strong non-uniform gradient up to $1/d^4$, with d as the distance between the field source and the exposed body. However, the fields couple poorly to the body, i.e. < –60 dB [25]. If it can be demonstrated that induced E-field by these local sources that are characteristic of the DUT is much less than 1 % of the compliance limit, it is not necessary to assess the local E-field.

When selecting a measurement system, the required performance, frequency response, and electromagnetic field strength range shall be considered.

6.1.2.2 Equipment for magnetic field strength measurements

Search-coil sensors are often used for a low frequency range of several hundred kilohertz and below. Different frequency bands can be covered by different sensors. In general, the search-coil probe is used for measuring environmental magnetic fields. The coil probe measures the induced voltage associated with the time-varying magnetic flux normal to the plane of the coil, averaged over the coil area. In a field that is uniform over the area of the coil, the induced voltage at the coil terminals is calculated according to Formula (18):

$$V = -\mathrm{j}\omega NBS \tag{18}$$

where

V is the induced voltage;

ω is the angular frequency (= $2\pi f$);

N is the number of turns;

B is the magnetic flux density (normal to the plane of the coil);

Documents
Document Sharing Hub

S is the cross-sectional area of the coil;

and all quantities are phasors.

The uncertainty of the measured field at the centre of the sensor caused by the gradient or other non-uniformities of the field shall be assessed (see also step f) of 6.1.1).

To achieve better sensitivity, the area and winding number are increased, and the magnetic flux density is enhanced by using ferromagnetic material in the core of the coil. The signal is processed to obtain flat frequency characteristics by an integrator in subsequent stages because the output is proportional to the frequency.

Magnetic field measurement equipment is divided into two classes: single-axis-probes with a single sensor, and three-axis-probes with three orthogonal sensors. IEC 61786-2 recommends using the three-axis type. The magnetic flux density of the three-axis component reading given in Formula (19) applies:

$$B_{\mathrm{R}} = \sqrt{B_x^2 + B_y^2 + B_z^2} \tag{19}$$

where B_x, B_y, and B_z are effective magnetic flux densities for the three orthogonal axes.

Three-axis magnetic field measurement equipment has the advantage of measuring the net field B_{R} regardless of the probe orientation.

6.1.2.3 Measurement equipment for the magnetic field gradient

The evaluation method based on the coupling factor as a function of the magnetic field gradient, i.e. 5.2.4.3, requires knowledge about the local B-field amplitude and gradient.

The magnetic field amplitude and gradient can be measured by sampling the field spatially in 3D around the location of exposure. The measurement can be performed by a single field sensor or multiple isotropic magnetic field sensors. A probe with a single sensor can be moved, e.g. by a robot system, to measure the field at separate locations of known spatial placement, if the test signal is repetitive and the phase relation can be established. A probe with multiple sensors can be used to measure the gradient directly, i.e. an axial or planar gradiometer [24], [26], [27], [28].

6.2 SAR and pE_{ind}

SAR and pE_{ind} can be measured and directly compared with the basic restrictions of the applicable requirement. The evaluation and validation procedures of internal electric field distribution and SAR measurements for wireless communication devices are specified in IEC/IEEE 62209-1528 (for the frequency range 4 MHz to 10 GHz). Similar measurement procedures can be used for WPT systems within the frequency range of 4 MHz to 30 MHz. In this document, only the deviations required to assess the spatial peak SAR values of WPT systems are specified. Clause B.4 specifies the procedures for probe calibration. Using an isotropic electric field probe, the SAR inside an irradiated body model can be determined. A SAR measurement system consists of a suitable phantom, an electric field probe, and a probe scanning system.

NOTE 1 The frequency limitation is given by the probe technology defined in IEC/IEEE 62209-1528:2020. As soon as other probes become available, the concept can directly be extended to frequencies below 4 MHz.

Documents
Document Sharing Hub

Full document details: BS EN IEC/IEEE 63184:2025

The physical characteristics of the phantom model (size, shape, electrical properties, etc.) shall simulate the human exposure condition by the DUT. Phantom models such as those specified in IEC/IEEE 62209-1528 may be used. The phantom model shall consist of materials with dielectric properties similar to humans. At a frequency lower than 30 MHz, the electrical properties of the material are dominantly affected by the conductivity of the material. The liquid specified in Table 2 or NaCl solution with the conductivity specified in Table 3 shall be used at frequencies between 0,1 MHz and 30 MHz. The relationship between conductivity and NaCl concentration is described in [29].

NOTE 2 The same requirements as in Table 2 are specified in IEC/IEEE 62209-1528:2020 for 4 MHz to 30 MHz.

The dependency of SAR on phantom properties and size are shown in Annex D. The same media may be used for frequencies below 4 MHz provided that the uncertainty with respect to conservative estimation is determined, considered, and documented (see 9.3.3).

NOTE 3 Reference [29] shows that the dielectric properties of saline solution differ by less than 5 % from their value at 1 GHz when the frequency tends to zero. This is why constant parameters are specified in Table 2 and Table 3 for the entire frequency range from 0,1 MHz to 30 MHz

Table 2 – Dielectric properties of the tissue-equivalent medium liquid

Frequency (MHz)	**Real part of the complex relative permittivity,** ε'_r (dimensionless)	**Conductivity,** σ (S/m)
0,1 to 30	55	0,75

Table 3 – Dielectric properties of the tissue-equivalent medium NaCl solution of 0,074 mol/L

Frequency (MHz)	**Real part of the complex relative permittivity,** ε'_r (dimensionless)	**Conductivity,** σ (S/m)
0,1 to 30	77	0,75

The DUT shall be operated at the closest accessible distance to the phantom. Due to the high SAR gradients of the induced field, measurements shall be performed with a known uncertainty of the field at the interface of the phantom shell to the liquid. An extrapolation method for the induced field may then be used to determine the SAR peak at the phantom surface. In that case, uncertainty due to the extrapolation method with respect to SAR values shall be included in the uncertainty budget.

NOTE 4 Examples for extrapolation methods are given in Annex E.

Extensions of the area scan or volume scan procedures may be used to determine the location of maximum SAR. Subclause 7.4 of IEC/IEEE 62209-1528:2020 specifies the scanning procedures. The scanning region shall be 20 % larger than the source or as large as the phantom, whichever is smaller. Additional zoom scans shall be measured for secondary peaks if the primary peak is within 2 dB of the SAR limit.

NOTE 5 Refer to applicable national regulations for the specified SAR limit.

The zoom scan parameters shall be those of Table 4 of IEC/IEEE 62209-1528:2020 and shall meet the requirements given in steps 3 through 5 of 7.4.2 of IEC/IEEE 62209-1528:2020.

Documents
Document Sharing Hub

Full document details: BS EN IEC/IEEE 63184:2025

The pE_{ind} can be derived from the measured local maximum SAR value in the phantoms standardized in IEC/IEEE 62209-1528 using Formula (20):

$$pE_{\text{ind}} = \sqrt{pSAR \times \frac{\rho}{\sigma}} \tag{20}$$

where

pE_{ind} is the maximum E-field at the phantom surface;

$pSAR$ is the local specific absorption rate;

σ is the conductivity;

ρ is the equivalent tissue density of 1 000 kg/m^3 to account for the actual density of brain or body tissue.

The maximum instantaneous E-field value at the phantom surface $pE_{\text{ind,inst}}$ is then given by Formula (21):

$$pE_{\text{ind,inst}} = pE_{\text{ind}}\sqrt{PAR} \tag{21}$$

where

$pE_{\text{ind,inst}}$ is the maximum instantaneous E-field at the phantom surface;

pE_{ind} is given in Formula (20);

PAR is the signal peak power to average ratio.

6.3 Contact currents

6.3.1 General

Subclauses 6.3.2 and 6.3.3 describe equipment and measurement protocol for the assessment of contact currents. IEC TR 63167 [22] provides general information related to human exposure to electric, magnetic, and electromagnetic fields including assumed situations and a proposed method for measuring contact currents.

6.3.2 Equipment

An electrical equivalent circuit human body impedance model, which is frequency dependent, is used to measure contact currents. Figure 7 shows an equivalent circuit, as depicted in IEC 60990 [30], which simulates a human body. Several other studies have evaluated human body impedance and proposed more precise equivalent circuits using arrangements of resistors and capacitors [31], [32], [33], [34]. The frequency characteristics of human body impedance with grasping conditions are compared in Figure 8. The impedance depends on area of contact and usually the impedance for grasping contact is lower than that for point contact.

NOTE The assumed conditions of contact are "point contact" (area not specified) in ICNIRP guidelines [4], [5], and "touch contact" with a contact area of 1 cm^2 and "grasping contact" with a contact area of 15 cm^2 for IEEE safety guidelines [8]).

Figure 9 shows the configuration of a contact current meter. The contact terminal is made of metal. If the target point of the contact part is painted, a 10 cm × 20 cm metal foil should be attached to it to simulate a hand palm contact, according to IEC 60990 [30]. A metal board equivalent to the size of a foot is used as the ground electrode. The contact current is measured from the current flowing through the equivalent circuit of the human inside the meter.

AVA Documents Document Sharing Hub

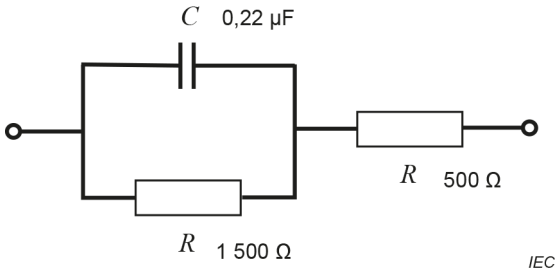

Figure 7 – Human body equivalent circuit proposed in IEC 60990 [30]

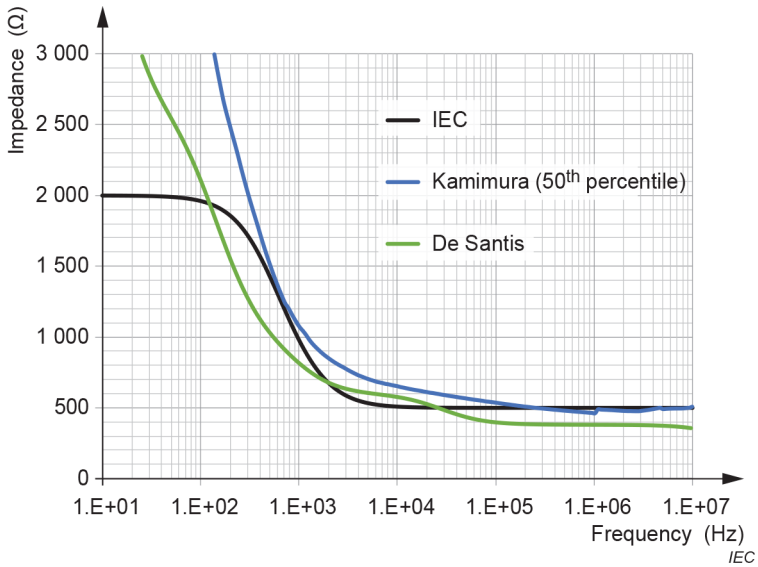

Figure 8 – Impedance frequency characteristics of adult male and equivalent circuits proposed in IEC 60990 [30] and evaluated values [31], [32], [33], [34]

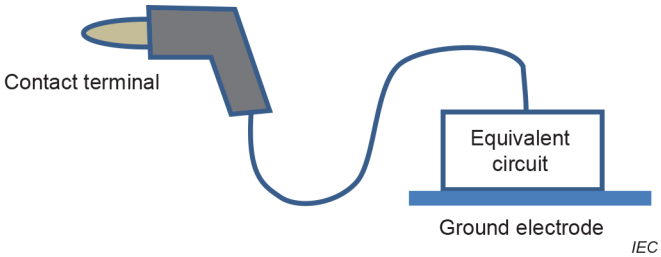

Figure 9 – Example of contact current measurement equipment

6.3.3 Measurements

The following issues shall be considered for the measurement of contact currents:

- Avoid electromagnetic field disturbances caused by the operator and measurement systems as much as possible.
- Environmental conditions (temperature, humidity, vibration, electromagnetic fields, etc.) can affect the measurement equipment.
- The requirements on the measurement equipment shall be specified or the reference to an appropriate document, e.g. IEC TR 63167:2018 [22], shall be included.
- A calibrated measurement system shall be employed.

Documents
Document Sharing Hub
Full document details: BS EN IEC/IEEE 63184:2025

There are two types of measurements, specified in the following a) and b), depending on the expected exposure scenario.

The measurement equipment specification, exposure scenario and its contact current shall be reported.

a) Measurement methods using an ungrounded metal board (simulating the EV body):
   1) Place a ground electrode where a person can stand.
   2) Place an ungrounded metal board large enough at the location where metal objects can exist in the actual usage condition. For representing an EV, a metal board larger than 1,2 m × 1,2 m may be used (see Figure I.10). Choose the closest position in the actual usage because the contact current tends to become higher as metal objects come closer to the DUT. Find the maximum condition of the contact current because the metal board position (height) and direction can change the contact current strength.
   3) Touch the contact terminal to the metal board. Find the maximum reading on the meter over multiple touch locations if there is a dependency on the touch position.

b) Measurement methods using a grounded metal board:
   1) Place a grounded metal board large enough to cover all metal objects that may exist in the actual usage condition. Choose the closest position in the actual usage because the contact current tends to become higher as metal objects come closer to the DUT. Find the maximum position of the contact current because the metal board position (height) and direction can change the contact current strength.
   2) Touch the contact terminal to the metal board where a person can touch (see Figure I.9). The contact current becomes larger according to the magnitude of the interlinkage magnetic flux to a loop created by the grounded metal board and human body. A rectangular loop with size of minimum 1,5 m (height) × 0,5 m (width) shall be used to evaluate the contact current. Find the loop arrangement which gives the maximum contact current value.

Additional information on the measurement of contact currents can be found in IEC 60990:2016 [30].

7 Computational assessment methods

7.1 General

The internal electric field pE_{ind}, the psSAR, or whole-body SAR for comparison with basic restrictions is calculated by simulation using a representative set of anatomical human models.

NOTE 1 As an example for a representative set, twelve models were used in [35] to derive general coverage factors.

Calculations may be performed using full wave methods or quasi-static methods, depending on the electrical size of the problem geometry. For quasi-static problems, the effect of the induced fields in the human body on the incident field source is assumed to be negligible. The incident fields and the induced fields can be evaluated in separate simulations using different computational methods. For the calculation of the incident fields, analytical or quasi-analytical methods can be applicable. Table 4 summarizes the computational methods for exposure evaluation. A brief description of computational methods is also given in Annex F. Annex H specifies averaging algorithms, and code verification and model validation. At present, body phantoms to conservatively measure the exposure to WPT systems are not available. These models shall include the following:

- availability of larger bodies which have increased absorption rates and are therefore more susceptible to electrostimulation effects from low frequency magnetic fields;
- availability of smaller bodies (children) which can be closer to the field source;
- individual segmentation of the tissues of the central and peripheral nervous systems for evaluation with the respective basic restrictions;

AVA Documents Document Sharing Hub

- posable or movable limbs for the modelling of realistic exposure scenarios.

All computational algorithms shall be verified for technically correct implementation. Guidance is provided in Annex H.

NOTE 2 The measurement standard IEC/IEEE 62209-1528:2020 specifies SAR measurement methods for a frequency range from 4 MHz to 10 GHz. While a frequency range of 30 MHz to 6 GHz is specified for the computational standards IEC/IEEE 62704-1:2017 and IEC/IEEE 62704-4:2020, the computational methods are generally independent of the frequency. They are applicable for the frequency range of this document provided that the uncertainty of the truncation of the computational domain is appropriately considered and its uncertainty assessed.

Table 4 – Computational methods

Calculation method	Note
BEM (boundary element method)	Full-wave computation
FDFD (finite difference frequency domain)	Full-wave computation
FDTD (finite difference time domain)	Full-wave computation
FEM (finite element method)	Full-wave or quasi-static approximation computation
QS-FDTD (quasi-static finite difference time domain)	Quasi-static approximation computation
FIT (finite integration technique)	Full-wave or quasi-static approximation computation
MoM (method of moments)	Full-wave computation
Hybrid method (e.g. MoM + FDTD)	Full-wave computation
SPFD (scalar potential finite difference)	Quasi-static approximation computation
IM (impedance method)	Quasi-static approximation computation

7.2 Quasi-static approximation

For the applicability of a computational method based on the quasi-static approximation, the upper frequency limit is established considering the dimensions of the exposed body region or person, the size of the field source, and the distance between them. The frequency limit is then given by the quasi-static approximation of Formula (22), Formula (23), and Formula (24):

$$\left|\omega^2 \varepsilon \mu D^2\right| << 1 \quad \Leftrightarrow \quad \left(\frac{D}{\lambda}\right)^2 << 1 \tag{22}$$

or

$$\omega^2 \Re\{\varepsilon\} \mu D^2 << 1 \tag{23}$$

and

$$\omega \sigma \mu D^2 << 1 \tag{24}$$

Documents
Document Sharing Hub
Full document details: BS EN IEC/IEEE 63184:2025

where

ω is the angular frequency;

$\Re\{\varepsilon\}$ is the real part of the complex relative permittivity of the exposed tissue or the tissue-equivalent medium;

μ is the permeability;

λ is the minimum wavelength within the exposed region;

σ is the conductivity of the exposed tissue or the tissue-equivalent medium;

D is the feature size, which encompasses the dimensions of the field source and the exposed body or phantom considering the reduction of the wavelength due to the presence of dielectrics with a relative permittivity greater than 1.

Formula (22), Formula (23), and Formula (24) contain only the frequency, the dielectric and magnetic properties, and spatial dimensions of the geometry to be analysed (field source and exposed body). They apply to both electric and magnetic field exposure. The frequency range within which electric and magnetic fields can be regarded as decoupled is identical for electric and magnetic field exposure. Hence, the quasi-static approximation applies to both inductive and capacitive coupling.

A rationale shall be given along with evaluation results on why the quasi-static approximation applies on the evaluated exposure scenario. Possible deviations from a full wave solution shall be discussed and should be considered in the uncertainty budget (9.3).

7.3 Computational assessment against the basic restrictions

7.3.1 General

The basic restrictions on human exposure are specified in terms of:

- peak spatial average SAR [3], [8] (7.3.2);
- whole-body average SAR [3], [8] (7.3.3);
- averaged current density on a surface [4] (Clause G.1);
- peak spatial average E-field in a cubical volume [5] (Clause G.2);
- peak spatial average E-field along a line [8] (G.2.3);
- maximum local E-field [36] (G.2.4).

Different limits can apply for these quantities depending on the exposed body region. The computational code or the applied post-processing techniques shall implement the required averaging methods. Because the descriptions of the averaging algorithms in the exposure guidelines that establish them are generally not sufficiently detailed for an implementation as a computational algorithm, this document refers to the respective computational International Standards that specify those or specifies its own algorithms if an appropriate definition is not available elsewhere. Details are given in 7.3.2, 7.3.3, and Annex G. The implementation of these algorithms shall be validated according to the methods specified in Annex H.

Peak quantities, such as the pE_{ind} or the $psSAR$, can be read out directly from the post processor. Alternatively, the methods specified for the peak spatial average quantities may be applied (7.3.2, Clause G.2) with averaging volumes on the order of magnitude of the voxels or tetrahedra of the exposed body region. Care should be taken concerning stair-casing artefacts because these may affect the readout of the global field maximum or be dominant in small averaging volumes.

Documents
Document Sharing Hub

Full document details: BS EN IEC/IEEE 63184:2025

7.3.2 Peak spatial-average SAR

The peak spatial average SAR shall be evaluated according to IEC/IEEE 62704-1 for Cartesian meshes, and according to IEC/IEEE 62704-4 for unstructured meshes.

NOTE The computational methods specified in IEC/IEEE 62704-1 and IEC/IEEE 62704-4 are independent of the frequency at which the psSAR is evaluated.

7.3.3 Whole-body average SAR

The whole-body average SAR shall be evaluated according to IEC/IEEE 62704-1 for Cartesian meshes, and according to IEC/IEEE 62704-4 for unstructured meshes.

NOTE The computational methods specified in IEC/IEEE 62704-1 and IEC/IEEE 62704-4 are independent of the frequency at which the whole-body SAR is evaluated.

7.3.4 Averaged current density on a surface

The electric field distribution in the exposed body shall be evaluated according to IEC/IEEE 62704-1 for Cartesian meshes, and according to IEC/IEEE 62704-4 for unstructured meshes. The averaged current density shall then be calculated according to Clause G.1.

NOTE The computational methods specified in IEC/IEEE 62704-1 and IEC/IEEE 62704-4 are independent of the frequency at which the electric field is evaluated.

7.3.5 Peak spatial average internal E-field in a cubical volume

The electric field distribution in the exposed body shall be evaluated according to IEC/IEEE 62704-1 for Cartesian meshes, and according to IEC/IEEE 62704-4 for unstructured meshes. The peak spatial average E-field in a cubical volume shall then be calculated according to Clause G.2.

NOTE The computational methods specified in IEC/IEEE 62704-1 and IEC/IEEE 62704-4 are independent of the frequency at which the electric field is evaluated.

7.3.6 Peak spatial average internal E-field along a line

The electric field distribution in the exposed body shall be evaluated according to IEC/IEEE 62704-1 for Cartesian meshes, and according to IEC/IEEE 62704-4 for unstructured meshes. The peak spatial average E-field along a line shall then be calculated according to G.2.3.

NOTE The computational methods specified in IEC/IEEE 62704-1 and IEC/IEEE 62704-4 are independent of the frequency at which the electric field is evaluated.

7.3.7 Maximum local internal E-field

The electric field distribution in the exposed body shall be evaluated according to IEC/IEEE 62704-1 for Cartesian meshes, and according to IEC/IEEE 62704-4 for unstructured meshes. The maximum local E-field shall then be calculated according to G.2.4. It should be noted that several simulations with different mesh resolutions according to IEC/IEEE 62704-1 or IEC/IEEE 62704-4 should be used to reduce the impact of staircasing errors.

NOTE The computational methods specified in IEC/IEEE 62704-1 and IEC/IEEE 62704-4 are independent of the frequency at which the electric field is evaluated.

Documents
Document Sharing Hub

Full document details: BS EN IEC/IEEE 63184:2025

8 Combination of measurement and computational methods for inductive WPT systems

8.1 General

Because internal electric field, current density, and SAR are difficult to measure directly, the evaluation is often performed using computational approaches. However, it is difficult to accurately model an actual exposure situation in simulations including an electric vehicle body, ground planes, etc. In addition, it is sometimes difficult to retrieve information about the size, shape, and design of the WPT systems. It is possible to evaluate internal electric field or SAR by an approach combining both the measurement of electromagnetic fields around the system and computational analyses of induced quantities. The magnetic near-field data are first measured in the area occupied by the human body. Then, the measured magnetic fields are used as incident fields in an applicable computational method (Table 4) to derive the internal electric field strength inside the human-body model.

8.2 Measurement of magnetic field

For measurements of magnetic field distributions below 30 MHz, search-coil sensors are often used. Both amplitude and phase of the magnetic field shall be measured in the area occupied by the human body. To measure the phase of magnetic field, one magnetic sensor is fixed at a specific position to retrieve the reference phase, and the other sensor is moved over the area occupied by the human body.

8.3 Computational analyses of induced quantities

Anatomical human models or appropriate dosimetric phantoms shall be used to calculate induced field quantities. Computational methods for the calculation of the induced field quantities are summarized in Annex F. The measured magnetic field distribution is applied as the incident field in an applicable computational method (Table 4). The measured magnetic field data may be directly applied as a source with some computational methods. However, those computational methods that use vector potentials as a source to calculate the internal electric field require the reconstruction of vector potentials from the measured magnetic field ($\boldsymbol{H}$) or the magnetic flux density ($\boldsymbol{B}$) [37]. A finite number of samples of B from measurements may be used for field reconstruction taken at monitor points. In this case the spatial coordinate of the collected measurement samples is also needed.

The procedure to reconstruct the B-field distribution is specified in [37]. The magnetic flux density is assumed to be $\boldsymbol{B} = u_x B_x + u_y B_y + u_z B_z$, which satisfies $\nabla \cdot \boldsymbol{B} = 0$, where $u_{x,y,z}$ are unit vectors. Hence it can be represented using a vector potential $\boldsymbol{A}$, so that $\nabla \times \boldsymbol{A} = \boldsymbol{B}$. A vector potential is given by Formula (25), Formula (26), and Formula (27):

$$A_x = -\int_0^y \left[\frac{1}{3} B_z(x,y',z) + \frac{1}{6} B_z(x,y',0)\right] \mathrm{d}y' + \int_0^z \left[\frac{1}{3} B_y(x,y,z') + \frac{1}{6} B_y(x,0,z')\right] \mathrm{d}z' \tag{25}$$

$$A_y = -\int_0^z \left[\frac{1}{3} B_x(x,y,z') + \frac{1}{6} B_x(0,y,z')\right] \mathrm{d}z' + \int_0^x \left[\frac{1}{3} B_z(x',y,z) + \frac{1}{6} B_z(x',y,0)\right] \mathrm{d}x' \tag{26}$$

$$A_z = -\int_0^x \left[\frac{1}{3} B_y(x',y,z) + \frac{1}{6} B_y(x',0,z)\right] \mathrm{d}x' + \int_0^y \left[\frac{1}{3} B_x(x,y',z) + \frac{1}{6} B_x(0,y',z)\right] \mathrm{d}y' \tag{27}$$

Documents
Document Sharing Hub
Full document details: BS EN IEC/IEEE 63184:2025

Formula (25), Formula (26), and Formula (27) require that the vector components of the magnetic flux density be known. Therefore, they are valid for any arbitrary inhomogeneous, anisotropic, or nonlinear medium. In free space, the vector components of the magnetic flux density can be calculated directly from the H-field vector.

8.4 Computational assessment against the basic restrictions

The basic restrictions are generally specified for induced field quantities that are averaged over a certain geometrical shape in the exposed body or phantom for the computational assessment of the induced fields, e.g. pE_{ind} and $psSAR$. The methods described in 8.3 shall be applied to calculate the induced fields for a representative set of anatomical models of the human body or an appropriate dosimetric phantom. Computation of the induced fields against the basic restrictions shall then be carried out according to 7.3.

NOTE Some national regulations specify peak values instead of averaged quantities as basic restrictions on the induced fields.

9 Uncertainty assessments

9.1 General

In 9.2 to 9.4, the sources of measurement and computational uncertainty are listed. Their contributions to the uncertainty shall be assessed for the evaluation of the total uncertainty. The uncertainty budget is based on the concepts of ISO/IEC Guide 98-1 [38], ISO/IEC Guide 98-3 [39], [40], and [41]. For most methods specified in this document, each source of uncertainty is considered as independent and can therefore be assessed separately from the others.

9.2 Measurement methods

9.2.1 Measurement uncertainty budget

Table 5 summarizes the main parameters related to magnetic field measurements.

Table 5 – Example of uncertainty evaluation of the the E-field and H-field exposure assessment using measurement methods

Quantity x_i (source of uncertainty)	Reference	Prob. dist.[a]	Unc.	Divisor[a] q	Standard uncertainty $u(x_i)$	Sensitivity c_i	Expanded uncertainty $u_i(y)$	Degrees of freedom v_i
Amplitude calibration uncertainty	9.2.2	N		1		1		
Probe anisotropy	9.2.3	R		√3		1		
Probe dynamic range linearity	9.2.4	R		√3		1		
Probe frequency domain response	9.2.5	R		√3		1		
Modulation response	9.2.6	R		√3		1		
Spatial averaging (maximum gradient)	9.2.7	R		√3		1		

Documents
Document Sharing Hub
Full document details: BS EN IEC/IEEE 63184:2025